FACTORS AFFECTING THE MEASUREMENTS OF PHOTOCHROMIC MATERIALS

Utkarshsinh Bhupendrasinh Solanki, M.Eng.

The Summary of the Dissertation thesis

Title of the dissertation:	**Factors Affecting the Measurements of Photochromic Materials**
Autor:	**Utkarshsinh Bhupendrasinh Solanki, M.Eng.**
Doctoral program:	**Textile Engineering**
Form of study:	**Full time**
Training department:	**Department of Material Engineering**
Supervisor:	**doc. Ing. Martina Viková, Ph.D.**

Composition of the dissertation defense committee:

Chairman:	
prof. Dr. Ing. Zdeněk Kůs	FT TUL, Department of Clothing Technology
Vice- Chairman:	
prof. Ing. Jakub Wiener, Ph.D.	FT TUL, Department of Material Engineering
prof. Ing. Radim Hrdina, CSc. (reviewer)	UPCE, Faculty of Chemical Technology, Department of Organic Materials Technology
prof. Ing. Josef Šedlbauer, Ph.D.	FP TUL, Department of Chemistry
doc. Ing. Ladislav Burgert, CSc.	University of Pardubice, Faculty of Chemical Technology
doc. Ing. Jiří Chvojka, Ph.D.	FT TUL, Department of Nonwovens and Nanofibrous Materials
plk. gšt. doc. Ing. František Racek, Ph.D.	University of Defense in Brno, Faculty of Military Technology

The second reviewer, who is not a member of the committee:

Aravin Prince Periyasamy, M.Sc., Ph.D. VVT Technical Research Centre of Finland

The dissertation can be consulted at the Department of Doctoral Studies, Faculty of Textile Engineering, Technical University of Liberec.

Liberec, 2026

ABSTRACT

Photochromic materials are widely investigated for advanced applications, including UV sensors, optical data storage, stimuli–responsive materials, and visual displays. In textile implementations, however, their practical use is limited by low lightfastness under UV activation, which manifests as photofading, photodegradation, and performance loss during repeated switching. A further challenge is the lack of standardized and reproducible protocols for quantifying photofading and photofatigue in solid–state photochromic systems.

This dissertation investigates the UV–driven photokinetics and photodegradation of textile–based photochromic systems prepared using a spiroxazine–family dye, 5–chloro–1,3,3–trimethylspiro[indoline–2,3′–(3H)naphtho(2,1–b)(1,4)–oxazine]. Two fabrication routes were studied: (i) surface–applied photochromic prints produced by screen printing and (ii) mass–dyed photochromic nonwovens produced via electrospinning–based dye–doping. Colourimetric characterisation was performed using FOTOCHROM3 (360 nm) and FOTOCHROM2 (380 nm) systems. Spectral reflectance–time profiles were recorded at the dominant absorption wavelength of the coloured state (570 nm) and converted into *Kubelka–Munk* colour intensity units (K/S), enabling quantitative comparison of full photochromic cycles.

A response–based, stepwise measurement methodology was developed to quantify photofading once the system reached photosteady (photostationary) equilibrium and to evaluate the influence of key photodegradation parameters, including dye concentration, preparation route, irradiation time and intensity, UV dose, irradiation cycles (photofatigue), environmental conditions, measurement scenario within a cycle, and the excitation spectral power distribution (360 nm vs 380 nm). The photocolouration (exposure, E) and thermal fading (decay, D) phases were analysed independently. For the E phase, segmental linear regression of K/S versus $\log_{10}$(time) was applied to discriminate between one–phase (monexponential) and two–phase (bixponential) first-order kinetics, identified by a single linear segment or by two segments separated by a breakpoint. For the D phase, bleaching–state datasets were fitted using sigmoidal logistic functions – specifically, symmetric four–parameter logistic (4PL) and asymmetric five–parameter logistic (5PL) models. Nonlinear regression yielded plateau values, characteristic times, rate constants, and asymmetry coefficients, and goodness–of–fit was evaluated using the coefficient of determination (R^2).

Photochromic prints exhibited bi-exponential first-order kinetics during photocolouration and a symmetric sigmoidal (4PL) response during thermal fading. In contrast, photochromic nonwovens showed bi-exponential behaviour at low irradiance during photocolouration but transitioned to mono-exponential kinetics when irradiance was sufficient to reach the photostationary state; their thermal fading was best described by an asymmetric sigmoidal (5PL) response. Collectively, these results establish a unified kinetic framework for describing both growth and decay processes in solid–state photochromic textile systems, demonstrating that substrate architecture and irradiation conditions critically govern the apparent reaction mechanisms and degradation trajectories. The proposed protocol and kinetic models support robust design, qualification, and durability assessment of photochromic textiles for UV–sensing applications.

Keywords: photochromic dye; photofading; photodegradation; photochromic textiles; UV irradiance; *Kubelka–Munk* (K/S); UV sensor; first-order kinetics; 4PL/5PL logistic models; photofatigue

ABSTRAKT

Fotochromismus, významná oblast fotochemie, přitahuje značnou pozornost díky pokročilým aplikacím, jako jsou UV senzory, optické ukládání dat, materiály reagující na podněty a vizuální displeje. V textilních aplikacích je však jeho praktické využití omezeno nedostatečnou světlostálostí při UV aktivaci, která se projevuje jako foto–blednutí, fotodegradace a pokles výkonu při opakovaném přepínání. Dalším problémem je absence standardizovaných a reprodukovatelných protokolů pro kvantifikaci foto–blednutí a foto–únavy v pevné fázi fotochromních systémů.

Tato disertace zkoumá UV–řízenou fotokinetiku a fotodegradaci textilních fotochromních systémů připravených s využitím barviva ze skupiny spiroxazinů, 5–chloro–1,3,3–trimethylspiro[indoline–2,3′–(3H)naphtho(2,1–b)(1,4)–oxazine]. Byly studovány dvě výrobní cesty: (i) povrchově aplikované fotochromní tisky připravené sítotiskem a (ii) hmotově barvené fotochromní netkané textilie připravené metodou elektrostatického zvlákňování (electrospinning) s dopováním barviva. Kolorimetrická charakterizace byla provedena pomocí systémů FOTOCHROM3 (360 nm) a FOTOCHROM2 (380 nm). Časové profily spektrální reflektance byly zaznamenány při dominantní absorpční vlnové délce zbarveného stavu (570 nm) a převedeny do jednotek intenzity zbarvení podle *Kubelka–Munkovy* funkce (K/S), což umožnilo kvantitativní porovnání kompletních fotochromních cyklů.

Byla vyvinuta odezvově orientovaná, kroková metodika měření pro kvantifikaci foto–blednutí po dosažení foto–stacionárního (fotostacionárního) rovnovážného stavu a pro hodnocení vlivu klíčových parametrů fotodegradace, včetně koncentrace barviva, způsobu přípravy, doby a intenzity ozáření, UV dávky, počtu ozářecích cyklů (fotoúnava), environmentálních podmínek, měřicího scénáře v rámci cyklu a spektrálního rozložení výkonu excitačního zdroje (360 nm vs 380 nm). Fáze fotozbarvení (expozice, E) a tepelného blednutí (rozpad/útlum, D) byly analyzovány samostatně. Pro fázi E byla použita segmentová lineární regrese závislosti K/S na $\log_{10}$(čas), která umožnila rozlišit jednofázovou (monoexponenciální) a dvoufázovou (biexponenciální) kinetiku prvního řádu na základě přítomnosti jednoho lineárního úseku, resp. dvou úseků oddělených bodem zlomu. Pro fázi D byla data ve stavu odbarvování proložena sigmoidalními logistickými funkcemi, konkrétně symetrickým čtyřparametrovým logistickým modelem (4PL) a asymetrickým pětparametrovým logistickým modelem (5PL). Nelineární regrese poskytla hodnoty plató, charakteristické časy, rychlostní konstanty a koeficienty asymetrie a kvalita modelu byla posouzena pomocí koeficientu determinace (R^2).

Fotochromní tisky vykazovaly během fotozbarvení biexponenciální kinetiku prvního řádu a během tepelného blednutí symetrickou sigmoidalní odezvu popsanou modelem 4PL. Naproti tomu fotochromní netkané textilie vykazovaly ve fázi fotozbarvení biexponenciální chování při nízké irradianci, avšak při dostatečné irradianci, která umožnila dosažení fotostacionárního stavu, přecházely na monoexponenciální kinetiku; jejich tepelné blednutí bylo nejlépe popsáno asymetrickou sigmoidalní funkcí 5PL. Souhrnně tyto výsledky etablovaly jednotný kinetický rámec pro popis růstové i útlumové fáze v pevné fázi fotochromních textilních systémů a ukazují, že architektura substrátu a podmínky ozáření zásadně určují zdánlivé reakční mechanismy i degradační trajektorie. Navržený protokol a kinetické modely podporují robustní návrh, kvalifikaci a hodnocení životnosti fotochromních textilií pro aplikace UV senzorů.

Klíčová slova: fotochromní barvivo; fotoblednutí; fotodegradace; fotochromní textilie; UV irradiance; *Kubelka–Munk* (K/S); UV senzor; kinetika prvního řádu; logistické modely 4PL/5PL; fotoúnava

Annotation

This dissertation investigates UV-driven photokinetics and photodegradation in textile-based photochromic systems prepared with a spiroxazine dye (5-chloro-1,3,3-trimethylspiro[indoline-2,3′-(3H)naphtho(2,1-b)(1,4)-oxazine]). Two textile architectures were compared: (i) surface-applied photochromic prints produced by screen printing and (ii) mass-dyed photochromic nonwovens produced by electrospinning-based dye doping. Colourimetric characterisation was performed using FOTOCHROM3 (360 nm) and FOTOCHROM2 (380 nm). Reflectance–time profiles at the dominant coloured-state absorption wavelength (570 nm) were converted into *Kubelka–Munk* colour-intensity units (K/S), enabling quantitative comparison across complete photochromic cycles.

A response-based, stepwise methodology is proposed to quantify photofading at photostationary equilibrium and to evaluate the influence of key degradation parameters (dye concentration, preparation route, irradiance, exposure time, UV dose, cycling, environmental conditions, and excitation spectrum). The exposure (E) and thermal fading (D) phases were analysed independently using segmented linear regression (E phase) and logistic models (D phase; 4PL/5PL). Results show architecture-dependent behaviour: prints exhibit bi-exponential colouration and symmetric (4PL) fading, whereas nonwovens transition from bi-exponential to mono-exponential colouration with sufficient irradiance and show asymmetric (5PL) fading. Overall, the dissertation establishes dose-based kinetic descriptors and a consistent kinetic analysis protocol to support robust protocol design and durability assessment of photochromic textiles for UV-sensing applications.

Anotace

Tato disertace se zabývá UV-řízenou fotokinetikou a fotodegradací textilních fotochromních systémů připravených spiroxazinovým barvivem (5-chloro-1,3,3-trimethylspiro[indoline-2,3′-(3H)naphtho(2,1-b)(1,4)-oxazine]). Byly porovnány dvě architektury: (i) povrchově aplikované fotochromní tisky připravené sítotiskem a (ii) hmotově barvené fotochromní netkané textilie připravené metodou elektrostatického zvlákňování (electrospinning) s dopováním barviva. Kolorimetrická charakterizace byla provedena v systémech FOTOCHROM3 (360 nm) a FOTOCHROM2 (380 nm). Časové profily spektrální reflektance při dominantní absorpční vlnové délce zbarveného stavu (570 nm) byly převedeny do jednotek intenzity zbarvení podle *Kubelka–Munkovy* funkce (K/S), což umožnilo kvantitativní srovnání kompletních fotochromních cyklů.

Byla navržena odezvově orientovaná kroková metodika pro kvantifikaci fotoblednutí po dosažení fotostacionárního stavu a pro hodnocení vlivu klíčových parametrů degradace (koncentrace barviva, způsob přípravy, irradiance, doba ozáření, UV dávka, cyklování, podmínky prostředí a spektrum excitačního zdroje). Fáze fotozbarvení (E) a tepelného blednutí/útlumu (D) byly analyzovány samostatně pomocí segmentované lineární regrese (E) a logistických modelů 4PL/5PL (D). Výsledky potvrzují výraznou závislost na architektuře: tisky vykazují biexponenciální zbarvení a symetrické blednutí (4PL), zatímco netkané textilie přecházejí při dostatečné irradianci k monoexponenciální kinetice a jejich blednutí je nejlépe popsáno asymetrickým modelem 5PL. Práce zavádí dávkově (dose-based) definované kinetické deskriptory a harmonizovaný analytický postup pro návrh protokolů a hodnocení životnosti fotochromních textilií pro aplikace UV senzorů.

Summary

1. Introduction

Photochromic textiles are functional materials that reversibly change colour under light, enabling applications in adaptive clothing, visual indicators, UV dosimetry, sensing, and responsive textile systems. Unlike conventional dyed fabrics, photochromic textiles operate under dynamic conditions in which the observed optical signal depends not only on molecular switching reactions but also on the textile architecture and the measurement protocol. In real substrates, light transport, dye distribution, oxygen accessibility, and microstructural confinement strongly influence the apparent switching and fading behaviour.

Interpreting photochromism in textiles is fundamentally more complex than in homogeneous solutions or thin films. Textiles are optically thick, highly scattering, and structurally heterogeneous, producing depth-dependent attenuation and spatially non-uniform excitation. In addition, dyes reside in restricted microenvironments within coatings, fibres, and porous voids, where mobility and local polarity vary. These factors commonly drive deviations from idealised kinetics: colouration can show multi-regime growth rather than a single exponential rise, and thermal fading can be delayed, asymmetric, or long-tailed - effects that are especially pronounced in porous, volumetric architectures such as dyed nonwovens. As a result, simplified first-order models and single apparent rate constants often provide limited diagnostic value and cannot reliably distinguish architectures, dye loadings, or irradiation histories.

A key challenge is the nature of the measured signal. Textile photochromism is typically characterised by diffuse reflectance, so the response is an optical–photokinetic observable shaped by absorption and multiple scattering, not a direct concentration trace. The *Kubelka–Munk* colour strength function (K/S) is a practical proxy for colour intensity in scattering media, but its time dependence reflects the convolution of intrinsic photochemistry, architectural light transport, and protocol-defined boundary conditions. Robust evaluation therefore requires methods that explicitly accommodate this coupling.

Practical deployment is further limited by fatigue under repeated or sustained ultraviolet (UV) exposure. Although switching is nominally reversible, prolonged irradiation can cause irreversible transformations, accumulation of non-photoactive species, and progressive loss of colour intensity. These degradation processes depend strongly on architecture because optical path length, oxygen diffusion, and local dye concentration differ between surface-confined printed layers and volumetrically dyed fibrous nonwovens. Importantly, fatigue can alter not only response amplitude but also response shape, making intensity-only durability metrics insufficient.

This dissertation addresses these issues by developing a unified, operational framework for photochromic textiles that prioritises comparability and physical interpretability. The approach treats kinetic parameters as apparent, protocol-dependent descriptors and analyses photochromic cycles by separating exposure and decay phases, selecting model families based on trace shape. In parallel, photodegradation is assessed on a cumulative UV dose basis, enabling consistent comparison across irradiance levels and protocol structures within wavelength-specific contexts. Controlled experimental designs are used to evaluate the roles of relaxation phases, wavelength, dye loading, and architecture. By integrating unified kinetic analysis with dose-based fatigue assessment, the work bridges laboratory

characterisation and realistic performance evaluation, providing practical guidance for material screening, protocol design, and lifetime-oriented durability testing of photochromic textile systems.

2. Subject and Objectives of the Dissertation

This dissertation investigates photochromic behaviour in textile substrates, focusing on the kinetics of reversible colour switching and the mechanisms of irreversible photodegradation under sustained ultraviolet (UV) exposure. The work addresses textile systems in which the measured optical response arises from coupled effects of photochemistry, material architecture, and measurement protocol. Its central goal is to develop a robust, unified framework for evaluating photochromic performance in scattering textile media, where conventional kinetic interpretations are inadequate.

Two representative textile architectures are examined: (i) surface-confined photochromic prints produced by screen printing and (ii) volumetrically dyed photochromic nonwovens fabricated via dye incorporation during electrospinning. These architectures differ in dye distribution, optical path length, microstructural heterogeneity, and accessibility to oxygen/thermal relaxation, providing a controlled basis for determining how architecture governs apparent photocolouration, thermal fading, and long-term durability during repeated irradiation.

Because textile characterisation is based on diffuse reflectance, the recorded colourimetric response is an optical–photokinetic observable rather than a direct concentration trace. Accordingly, the study adopts an operational approach in which colour strength (K/S) is treated as the primary observable, and kinetic parameters are interpreted as apparent, protocol-dependent descriptors conditioned by irradiation history and boundary conditions. This perspective guides the analysis strategy and model selection throughout the dissertation.

2.1 Main Research Aim

To establish and validate a unified **kinetic** and **dose-based** evaluation framework for photochromic textiles that enables meaningful comparison of reversible switching and irreversible photodegradation across textile architectures, dye loadings, and irradiation protocols.

2.2 Specific Objectives

- Develop a unified kinetic analysis framework that accounts for the optical–photokinetic nature of diffuse reflectance measurements.
- Characterise exposure-phase (photocolouration) kinetics in prints and nonwovens using diagnostic, regime-based descriptors.
- Model decay-phase (thermal fading/bleaching) behaviour using appropriate sigmoidal families when relaxation deviates from ideal exponentials, including symmetry/asymmetry in the log-time domain.
- Quantify architecture-dependent kinetic differences between surface-confined and volumetrically dyed systems under controlled irradiation.
- Evaluate fatigue and photodegradation under sustained/repeated UV exposure using **cumulative dose** metrics.

- Determine how relaxation phases modulate recovery versus fragmentation during cycling.
- Assess the influence of wavelength, dye concentration, and textile microstructure on photodegradation in prints and nonwovens.

2.3 Research Hypotheses

- **H1 (Cumulative UV dose):** Fatigue is governed primarily by cumulative UV dose; dose-based analysis enables comparison across protocols.
- **H2 (Recovery–fragmentation):** Inclusion/exclusion of relaxation phases shifts recovery vs fragmentation, producing distinct fatigue trajectories.
- **H3 (Architecture discrimination):** Apparent descriptors from K/S–time profiles discriminate prints vs nonwovens due to differences in optical screening, dye distribution, and microenvironment.

3. Overview of the State of the Art

Photochromic dyes undergo reversible switching between optically distinct states (e.g., UV-induced coloured merocyanine and thermally/visibly driven recovery). While classical two-state, first-order descriptions are often adequate in dilute solutions or optically thin films, **solid and textile substrates** introduce restricted mobility, heterogeneous microenvironments, and depth-dependent excitation, which commonly produce **non-ideal growth and decay** behaviour (multi-regime build-up, delayed/long-tail relaxation, incomplete reversibility).

A central limitation in textile studies is that the measured signal is typically **diffuse reflectance**, not transmission; therefore, the response is an **optical–photokinetic observable** shaped by both absorption and multiple scattering. Your dissertation formalises the use of ***Kubelka–Munk* colour strength** ***(K/S)*** as the operational intensity index under fixed geometry, explicitly treating it as an effective observable rather than a direct concentration measure.

Kubelka–Munk colour strength

$$(K/S)_{\lambda,t} = f(R_{\lambda,t}) = \frac{(1-R_{\lambda,t})^2}{2R_{\lambda,t}} \qquad (2.1)$$

where, $R_{\lambda,t}$ is the measured spectral reflectance at wavelength λ, and K_λ and S_λ are the effective absorption and scattering coefficients, respectively.

Conventional kinetic fitting in solids often uses exponential models, but parameters can become ambiguous if reported as intrinsic constants without acknowledging scattering/protocol dependence. This dissertation work, therefore, frames mono-/bi-exponential forms as **effective descriptors** for segment-wise fitting (Exposure E, Decay D).

Mono-exponential (plateau approach):

$$(K/S)_t = (K/S)_\infty - [(K/S)_0 - (K/S)_\infty]e^{-kt} \qquad (2.2)$$

Bi-exponential (two-component effective response):

$$(K/S)_t = (K/S)_\infty - [(K/S)_0 - (K/S)_\infty][\beta e^{-k_1 t} + (1-\beta)e^{-k_2 t}] \quad (2.3)$$

where, k, k_1, and k_2 are apparent rate constants (s^{-1}) and β is the fractional contribution of the faster component ($0 \le \beta \le 1$).

To handle common non-ideal **multi-regime colour build-up**, the dissertation uses a **log-time diagnostic** $x = \log_{10} t$ and segmented linear representations to distinguish mono- vs bi-regime behaviour. A two-segment form with a breakpoint x_b is also defined.

Dose-based decline of cycle-wise colour response (photofading curve):

$$(K/S)_H = \left((K/S)_0 - (K/S)_\infty\right)\exp(-\alpha H) + (K/S)_\infty \quad (2.4)$$

where, $(\boldsymbol{K/S})_{\mathbf{0}}$ – initial upper plateau obtained after fitting the first UV irradiance cycle, $(\boldsymbol{K/S})_\infty$ – is the long–dose limiting plateau (the residual asymptote under sustained cycling), $\boldsymbol{\alpha}$ – photo–fading rate (m^2.Wh^{-1}), $(\boldsymbol{K/S})_{\boldsymbol{H}}$ – is the upper plateau obtained after a cumulative UV dose H (i.e., after successive growth–phase cycles). This representation provides a compact durability descriptor by linking the loss of achievable colouration directly to cumulative energy input.

3.1 Photochromic Switching in Solid-State Systems

Photochromic dyes reversibly interconvert between colourless and coloured forms; in ideal cases, recovery can be treated as first-order relaxation in the coloured-state fraction $u(t)$:

$$\frac{du}{dt} = -\mathrm{k}_{\mathrm{off}}\, u \Rightarrow u(t) = u_0 e^{-k_{\mathrm{off}} t} \quad (2.5)$$

In solid/textile substrates, switching is often **non-ideal** due to restricted mobility + heterogeneous microenvironments; a useful interpretation is **distributed-rate recovery** (superposition of exponentials):

$$u(t) = \int_0^\infty w(k)\; e^{-kt}\, dk \quad ; \int_0^\infty w(k)\, dk = 1 \quad (2.6)$$

where, w is a weighting function (a distribution of effective recovery rate constants)

3.2 Kinetic Descriptions of Photochromic Behaviour

Literature often reports “rate constants” from simple exponentials, but this becomes unreliable in heterogeneous solids/textiles; this dissertation work therefore uses **apparent/operational descriptors** rather than asserting intrinsic constants (especially for comparing architectures).

For the **exposure (E) phase**, your approach uses a **log-time diagnostic** with $x = \log_{10}(t)$ and linear/segmented regression as a robust descriptor of apparent build kinetics:

Single–segment representation (mono–regime):

$$(K/S)_t = a + b\, x \quad (2.7)$$

Two–segment representation (bi–regime):

$$(K/S)_t = \begin{cases} a_1 + b_1 x\,, & x \le x_b \\ a_2 + b_2 x\,, & x > x_b \end{cases} \qquad (2.8)$$

where, a_1, a_2 are intercepts of each segment; b_1, b_2 are the slope of correponding slopes

3.3 Optical–Photokinetic Coupling in Scattering Media

Textiles are strongly scattering, so the measured signal is an **optical–photokinetic observable**, not a direct concentration trace; colour is handled via the ***Kubelka–Munk* framework**, where K and S are effective absorption and scattering coefficients and $(K/S)_{\lambda^*,t}$ is the working intensity trace.

This coupling (UV penetration depth, inner-filter/self-screening, architecture-dependent path lengths) is a key reason why solution-style kinetics can mislead when applied directly to textiles.

3.4 Fatigue and Photodegradation in Photochromic Textiles

Textile durability is limited by irreversible pathways under UV exposure; your dissertation treats **cumulative UV dose** as the primary comparison variable: H (cumulative dose) with irradiance E and protocol-defined cycling terms.

Photofading/photodegradation is then expressed **dose-based** (rather than just time/cycle-count), using a log-intensity formulation of the form:

$$-(\log I - \log I_0) = \alpha H \qquad (2.9)$$

3.5 Key limitations motivating this dissertation

- **Idealised kinetics** are overused despite optical–photokinetic coupling in textiles.
- **Non-ideal growth/decay** in heterogeneous substrates is treated inconsistently.
- **Operational descriptors** for cross-architecture comparison are rarely standardised.
- Fatigue studies often ignore **cumulative UV dose** and **protocol structure**, limiting comparability across irradiance/wavelength/protocols.

4. Experimental and Methodological Framework

This section outlines the experimental design and analysis workflow used to evaluate photochromic switching and UV-induced fatigue in textile substrates. The description is intentionally operational and focuses on the elements required to interpret the kinetic and photodegradation results.

4.1 Materials and Textile Architectures

Two contrasting textile architectures were used to represent fundamentally different optical and microstructural environments:

- **Surface-confined photochromic prints (screen printed):** dye concentrated near the textile surface in a relatively uniform layer, giving a short effective optical path length and reduced depth-dependent attenuation while retaining textile scattering.
- **Volumetrically dyed photochromic nonwovens (electrospun):** dye incorporated into the polymer solution prior to electrospinning, producing porous, heterogeneous fibrous structures with volumetric dye distribution. Dye loading was systematically varied (low vs high) to quantify concentration-driven optical screening, aggregation, and constraint-dominated kinetics.

This paired-architecture design enables direct isolation of how dye distribution and textile structure control apparent switching, fading, and durability.

4.2 Measurement Instrumentation and Irradiation Conditions

Photochromic response was measured using dedicated spectrophotometric setups combining controlled UV activation with diffuse reflectance acquisition. Switching and degradation were primarily evaluated at **360 nm** and **380 nm** to probe wavelength effects using FOTOCHROM3 and FOTOCHROM2 spectrophotometers, respectively. Temperature and visible-light conditions were controlled to ensure reproducible decay measurements and to separate thermal fading from photochemical contributions. Accelerated ageing used a **xenon solar simulator** to approximate broadband outdoor exposure. Protocol variables (irradiance, exposure time, relaxation duration) were held constant within each series to preserve comparability.

4.3 Colourimetric Data Treatment

Diffuse reflectance spectra were converted to colour strength using the ***Kubelka–Munk*** function, which is treated as an **operational intensity proxy** in scattering textiles rather than a direct concentration measure. Analysis, therefore, emphasised relative changes in K/S with time, cycle number, and cumulative dose to compare switching speed, attainable colour intensity, reversibility, and fatigue. Where needed, segment-wise normalisation was applied to reduce baseline/scattering offsets and improve cross-sample comparison while preserving kinetic shape.

4.4 Segmentation of the Photochromic Cycle

Each cycle was analysed in two operational phases:

- **Exposure phase (E):** UV-induced photocolouration (generation of coloured form).

- **Decay phase (D):** thermal and/or visible-light-driven fading (relaxation toward the initial state).

This separation reflects distinct boundary conditions and allows phase-appropriate modelling without conflating different processes.

4.5 Modelling Philosophy and Descriptor Selection

The analysis adopts a conservative, diagnostic-driven approach: model families are chosen to match trace features rather than enforcing a single mechanistic model. Exposure behaviour is classified using linearised diagnostics to distinguish **mono-regime vs multi-regime** growth, while decay behaviour is modelled using **logistic/sigmoidal functions** when relaxation deviates from ideal exponentials. Extracted parameters (apparent rates, characteristic times, plateaus, asymmetry factors) are reported as **protocol-conditional descriptors**, supporting robust comparisons across architectures, dye loadings, and irradiation histories, and enabling the identification of non-ideal behaviour arising from optical screening, heterogeneity, or fatigue distortion.

5. Unified Kinetics of Photochromic Colouration and Thermal Fading

5.1 Rationale for a Unified Kinetic Interpretation

Kinetic evaluation of photochromic textiles cannot rely on conventional solution/thin-film models because the measured response is a **coupled optical–photokinetic signal** in a scattering, heterogeneous medium. The apparent behaviour $K/S_{(t)}$ reflects not only intrinsic switching chemistry but also **architecture-dependent optical screening**, depth-dependent excitation, and protocol boundary conditions.

To enable meaningful comparison across architectures, dye loadings, and irradiation protocols, this dissertation adopts a **unified, diagnostic-driven** interpretation. Rather than enforcing a single mechanistic model, it extracts **operational kinetic descriptors** that preserve sensitivity to genuine material/architectural differences while avoiding interpretation of fitted parameters as intrinsic molecular constants.

A key premise is strict separation of the photochromic cycle into two segments with different boundary conditions: **Exposure (E)** under UV ON (photoconversion under continuous excitation) and **Decay (D)** under UV OFF (thermal/visible relaxation via distributed pathways). Treating both phases with a single model obscures trace-shape differences and yields ambiguous parameters.

Architecture strongly shapes apparent kinetics. **Surface-confined prints** have short optical path lengths and relatively accessible dye populations, often producing near-ideal growth and more symmetric decay in log-time. **Volumetrically dyed nonwovens** exhibit depth-dependent attenuation, heterogeneous microenvironments, and restricted mobility, leading to distorted growth/decay profiles—effects amplified at high loadings by inner-filtering and aggregation.

Accordingly, the framework selects model families based on trace diagnostics: exposure is analysed using linearised/segmental methods to resolve regime structure, and decay is modelled with logistic families when relaxation deviates from simple exponentials, including explicit treatment of asymmetry in log-time.

Finally, applying the same descriptors across cycles and cumulative UV dose links reversible kinetics to fatigue: photodegradation changes both **amplitude** and

shape of E and D responses, allowing fatigue-driven distortion to be tracked and separated from protocol artefacts. This forms the basis for evaluating **H3 (architecture discrimination)** in the following sections.

5.2 Exposure Phase (E): Photocolouration Kinetics

The exposure phase (E) corresponds to UV-driven photocolouration, where the colourless dye converts to the coloured merocyanine form. Although idealised systems under uniform irradiation can often be approximated as a first-order approach to a photostationary state, textile substrates frequently deviate from this approximation due to **optical screening, heterogeneous dye microenvironments, and non-uniform (depth-dependent) excitation**. Therefore, exposure kinetics must be evaluated diagnostically rather than described by a single universal model.

In this dissertation, photocolouration is analysed using a **linearised, segment-based approach** applied to K/S–*time* traces under fixed irradiation conditions. Where required, traces are **normalised** to reduce baseline offsets and architecture-dependent scattering differences, improving cross-sample comparability while preserving kinetic shape and enabling discrimination between **mono-regime** and **multi-regime** growth behaviour.

5.2.1 Diagnostic Framework for Exposure-Phase Analysis

Exposure traces are first screened for **curvature, inflection points, and slope changes** indicative of regime transitions. The **normalised** response is then linearised and tested against **mono-** and **bi-exponential** descriptions to classify growth as single- or multi-regime. Parameters are treated as **apparent, protocol-dependent descriptors**; the emphasis is on **regime structure**, **fast/slow contributions**, and **cycle-to-cycle stability**, not intrinsic rate constants.

This strategy (i) justifies a **single growth descriptor** when behaviour is near-ideal over the analysed window and (ii) identifies **multi-regime** cases driven by heterogeneity or optical screening that require architecture-aware interpretation.

5.2.2 Mono-Regime Versus Multi-Regime Growth Behaviour

- **Photochromic prints (surface-confined):** Exposure traces typically show a rapid rise in K/S followed by a smooth plateau. Over the practical time window, growth is often well represented by a **single apparent regime**; linearised diagnostics show little curvature and **cycle-stable** descriptors, consistent with a relatively uniform, optically accessible dye population.
- **Photochromic nonwovens (volumetric):** Exposure commonly shows **multi-regime growth**—a fast initial increase followed by a slower secondary regime—attributed to depth-dependent activation and heterogeneous microenvironments. This separation is most pronounced at **low dye loading**, where UV penetration is greater.
- **High-loaded nonwovens:** Exposure may appear **mono-regime**, but this reflects **constraint-dominated behaviour**: strong inner-filtering/aggregation suppresses contributions from deeper or slower populations. Apparent simplicity should therefore not be interpreted as true kinetic ideality.

5.2.3 Influence of Architecture and Dye Loading

Diagnostic analysis shows consistent architecture and loading trends. **Photochromic prints** display **higher apparent growth rates** and **more stable plateaus** than nonwovens under comparable irradiation, consistent with a shorter optical path length, lower attenuation, and a more uniform dye environment in the printed layer.

In **nonwovens**, **lower dye loading** increases UV penetration and strengthens the contribution of slower/deeper populations, producing more pronounced **multi-regime** growth. **Higher dye loading** increases inner-filtering/optical screening, reduces the effective excitation depth, and suppresses secondary regimes, leading to an **apparently simplified** (often monoregime) trace. These trends confirm that exposure kinetics must be interpreted jointly in terms of **architecture + optical coupling**, not by a single universal rate constant.

5.2.4 Exposure phase Implications for Unified Kinetic Interpretation

Exposure-phase behaviour in textiles cannot be compared using a single universal rate constant. **Regime structure and trace shape** carry the key diagnostic information because they reflect underlying **optical screening and microstructural constraints**. The unified, diagnostic-driven framework, therefore, enables consistent identification of **architecture-dependent** photocolouration behaviour and provides a robust basis for interpreting the subsequent decay-phase response.

The next section analyses the **decay phase (D)** using **logistic modelling** to capture the non-ideal relaxation behaviour characteristic of scattering textile substrates.

5.3 Decay Phase (D): Thermal Bleaching Kinetics

The decay phase (D) describes relaxation of the coloured merocyanine form back to the colourless state after UV is removed. While idealised systems are often approximated by a single first-order exponential decay, textile substrates commonly deviate from this approximation due to **distributed relaxation pathways**, **heterogeneous microenvironments**, and **protocol-defined boundary conditions**.

In scattering textiles, decay kinetics derived from K/S–*time* traces are a convolution of molecular relaxation, **optical attenuation, and architectural effects**. Consequently, decay curves can show **delayed onset**, **broad transitions**, and **log-time asymmetry**, which simple exponential models cannot capture without biasing parameter estimates or distorting the trace shape.

5.3.1 Rationale for Logistic Modelling of Decay Behaviour

When decay traces deviate from exponential behaviour, this dissertation models the decay phase using **sigmoidal logistic functions**, which capture relaxation governed by **distributed time constants** and gradual transitions between plateaus.

- **4PL** is used when decay is **symmetric in the log-time domain**.
- **5PL** is used when decay is **asymmetric**, with an added **asymmetry parameter** that quantifies the skewed, long-tail relaxation commonly observed in volumetrically dyed textiles.

Model choice is based on **trace-shape diagnostics**, not mechanistic assumptions. Logistic parameters are treated as **operational descriptors** (plateaus, midpoint/characteristic time, steepness, symmetry/asymmetry) to enable robust comparison across architectures and irradiation conditions.

5.3.2 Interpretation of Logistic Parameters as Apparent Descriptors

Logistic parameters are treated as **operational descriptors** of decay behaviour. The **upper and lower plateaus** represent the effective colour intensity at the start and end of the decay phase under fixed boundary conditions. The **midpoint time** provides a characteristic relaxation timescale, and the **steepness** parameter reflects how sharply the transition occurs.

For **asymmetric** decays, the **asymmetry parameter** quantifies skew toward faster or slower relaxation pathways, consistent with heterogeneous environments where one fraction relaxes quickly while another is stabilised/trapped within the textile matrix. Tracking these parameters over cycles or cumulative UV dose reveals fatigue effects on both **amplitude** and **decay shape**.

5.3.3 Architecture-Dependent Features of Decay Kinetics

- **Photochromic prints (surface-confined):** Decay is typically well captured by **a symmetric logistic (4PL)** model. More uniform dye environments and limited depth effects produce a relatively narrow relaxation-time distribution, giving **sharp, centred** transitions with little asymmetry.
- **Photochromic nonwovens (volumetric):** Decay is often **strongly asymmetric**, especially at higher loadings. Volumetric dye distribution, heterogeneous fibre microenvironments, and restricted mobility broaden and skew relaxation pathways, so **asymmetric logistic (5PL)** modelling is required to represent the long-tail behaviour without biasing the kinetics.

5.3.4 Role of Fatigue in Decay-Phase Distortion

Repeated or sustained UV exposure progressively distorts decay behaviour. Fatigue reduces attainable colour intensity and alters decay kinetics, typically seen as increased **midpoint time** and changes in **asymmetry**, indicating a growing contribution from slowly relaxing or partially non-reversible populations.

Using the same logistic model family across cycles allows direct tracking of these fatigue-induced shifts in decay shape, helping separate **reversible kinetic changes** from **irreversible photodegradation**. The following sections apply the exposure- and decay-phase framework to specific architectures and dye loadings, starting with photochromic prints.

5.4 Kinetic Behaviour of Photochromic Prints (100 g·kg^{-1})

Photochromic prints are a **surface-confined** architecture in which dye is concentrated in a thin, relatively uniform layer near the textile surface. This minimises depth-dependent attenuation and reduces microenvironmental heterogeneity compared with volumetrically dyed systems. Consequently, prints serve as a practical reference case for assessing how closely textile photochromic kinetics can approach idealised switching under scattering, textile-relevant measurement conditions.

5.4.1 Photocolouration (Exposure Phase): Segmental Linear Regression and Bi-Exponential Tendencies

In photochromic prints, UV irradiation produces a **rapid rise in colour strength** (K/S) followed by a smooth approach to a well-defined plateau. Linearised diagnostics show that, over the relevant time window, growth is typically captured by a single dominant regime, with cycle-stable apparent growth descriptors—consistent with a relatively homogeneous, optically accessible dye population. Minor short-term deviations (a small, fast component from a readily accessible surface dye) may appear, but they do not materially change the overall trace shape or plateau values. Therefore, for comparison purposes, print photocolouration can be represented using a single apparent growth descriptor. Across cycles within the studied dose range, fatigue in prints is expressed mainly as reduced attainable colour intensity rather than major distortion of exposure-phase kinetics, unlike nonwovens, where screening and heterogeneity strongly affect growth behaviour.

Table 5.1. Best-fit parameters and goodness-of-fit statistics for the growth (G) phase (top) and decay (D) phase (bottom) corresponding to **Figure 5.1**.

Best-fit values	Growth phase: **150E**600D_100g.kg^{-1}	Growth phase: **300E**600D_100g.kg^{-1}	Growth phase: **600E**600D_100g.kg^{-1}
Intercept a_1	3.938	4.485	3.984
Slope 1 b_1	1.737	1.318	1.628
Slope 2 b_2	0.2819	0.01388	-0.03941
Breakpoint x_b	1.411	1.665	1.567
t_b (s)	25.76	46.23	36.89
R^2	0.8281	0.7270	0.5862
Preferred model	**Segmental Linear Regression**	**Segmental Linear Regression**	**Segmental Linear Regression**

Best-fit values	Decay phase: 150E**600D**_100g.kg^{-1}	Decay phase: 300E**600D**_100g.kg^{-1}	Decay phase: 600E**600D**_100g.kg^{-1}
Hillslope (η)	-2. 107	-2.051	-2.343
Top plateau $(K/S)_\infty$	3.685	3.678	3.298
Bottom Plateau $(K/S)_0$	0.009018	0.009779	0.03431
t_{50} (s)	15.57	15.34	17.56
R^2	0.9947	0.9935	0.9962
Preferred model	**Sigmoidal (4PL)**	**Sigmoidal (4PL)**	**Sigmoidal (4PL)**

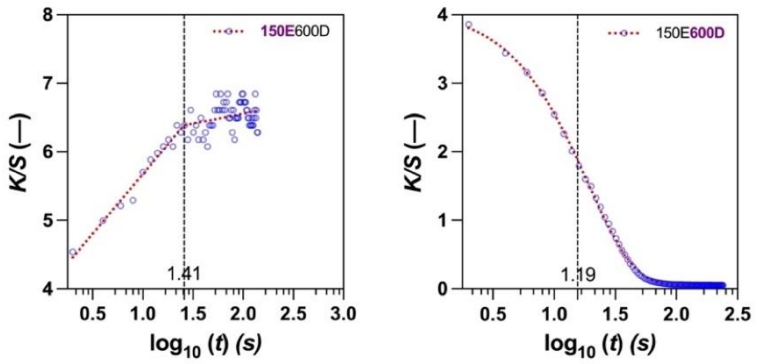

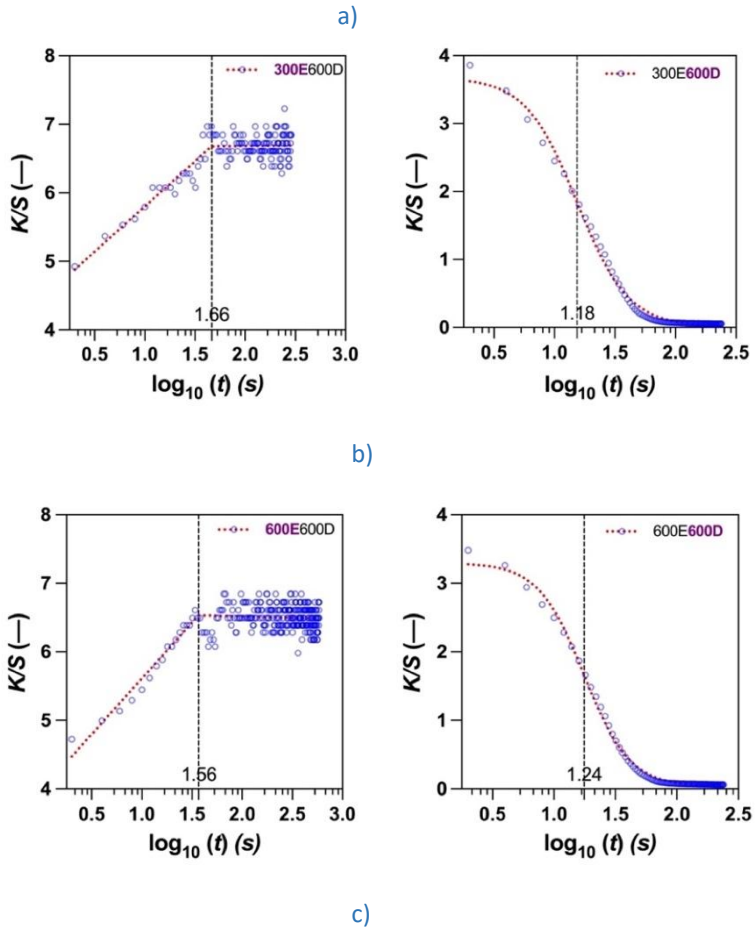

Figure 5.1. Experimental *K/S–time* data (blue) and best-fit model curves (red, dotted) for growth (G) and decay (D) of a photochromic print under three irradiance protocols: (a) 150E600D, (b) 300E600D, (c) 600E600D

5.4.2 Thermal Fading (D) Phase: Symmetric 4PL

Decay in photochromic prints shows a smooth, sigmoidal return toward the baseline after UV removal. In the log-time domain, the decay traces are largely **symmetric**, consistent with a relatively narrow distribution of relaxation times; therefore, **symmetric 4-parameter logistic (4PL)** models fit the data well.

The fitted parameters yield reproducible **upper and lower plateaus**, while **midpoint times** remain short with minimal drift across cycles, indicating that thermal recovery pathways in the printed layer are largely preserved under moderate UV exposure. The relatively sharp transition (steepness) further supports relaxation dominated by a comparatively uniform dye population. Overall, the success of symmetric 4PL modelling confirms that prints behave as a useful benchmark for comparison with more heterogeneous volumetric architectures.

5.4.3 Unified Interpretation of Growth–Decay Kinetics in Prints

Taken together, exposure and decay results show that photochromic prints exhibit a near-ideal textile kinetic signature**:** rapid, stable photocolouration followed by reproducible, symmetric (4PL) relaxation, with minimal cycle-to-cycle distortion of trace shape. When fatigue occurs, it appears mainly as **plateau (amplitude) loss** rather than major shifts in apparent rate behaviour. This does not imply solution-

like behaviour; rather, it indicates that in prints the effects of optical–photokinetic coupling and heterogeneity are sufficiently constrained to allow comparatively straightforward interpretation. Within the unified framework, prints therefore provide the **reference baseline** for identifying architecture-driven deviations in volumetric nonwovens and for validating **H3 (architecture discrimination)**.

5.5 Kinetic Behaviour of Low-Loaded Photochromic Nonwovens (10 g·kg⁻¹)

Low-loaded photochromic nonwovens are a **volumetrically dyed, porous fibrous architecture** with strong scattering, depth-dependent UV penetration, and highly heterogeneous dye microenvironments. These features produce distinctly non-ideal behaviour compared with surface-confined prints.

5.5.1 Photocolouration (Exposure Phase): Transition from Bi-Exponential to Mono-Exponential Behaviour

Exposure traces show clear **multi-regime photocolouration**: a rapid initial rise followed by a slower secondary regime, confirmed by linearised diagnostics (better described by **bi-exponential/segmented** behaviour than by a single mono-exponential). The fast component is associated with optically accessible near-surface populations, while the slower regime reflects progressive activation of deeper populations under attenuated UV. With increasing exposure or cumulative dose, the slower contribution can diminish, and the trace may appear **simplified (mono-regime)**. Importantly, this does not indicate increased homogeneity; it reflects the dominance of constrained and/or partially fatigued populations within the coupled optical–photokinetic system, so later-stage mono-regime behaviour must be interpreted cautiously.

Table 5.2. Best-fit parameters and goodness-of-fit statistics for the growth (G) phase (top) and decay (D) phase (bottom) corresponding to **Figure 5.2**.

Best-fit values	Growth phase: **720E**6000D_**1PP**	Growth phase: **1440E**6000D_**1PP**	Growth phase: **2880E**6000D_**1PP**	Growth phase: **6000E**6000D_**1PP**
Intercept a_1	0.06364	0.06057	0.08268	0.07178
Slope 1 b_1	0.02466	0.02978	0.005182	0.005296
Slope 2 b_2	0.006997	0.006478	-	-
Break point x_b	1.536	1.435	-	-
t_b (s)	34.35	27.22	-	-
R^2	0.8482	0.7881	0.6141	0.6611
Preferred model	**Segmental Linear Regression**	**Segmental Linear Regression**	**Linear Regression**	**Linear Regression**

Best-fit values	Decay phase: 720E**6000D_1PP**	Decay phase: 1440E**6000D_1PP**	Decay phase: 2880E**6000D_1PP**	Decay phase: 6000E**6000D_1PP**
Hillslope (η)	-4.460	-2.987	-3.205	-3.565
Skewness (α)	0.1706	0.2826	0.1658	0.1759
Top plateau $(K/S)_\infty$	0.09873	0.1057	0.08274	0.07734
Bottom Plateau $(K/S)_0$	0.03737	0.04312	0.03921	0.04287
t_{50} (s)	40.77	41.27	39.72	56.83
R^2	0.9678	0.9699	0.9405	0.9104
Preferred model	**Sigmoidal (5PL)**	**Sigmoidal (5PL)**	**Sigmoidal (5PL)**	**Sigmoidal (5PL)**

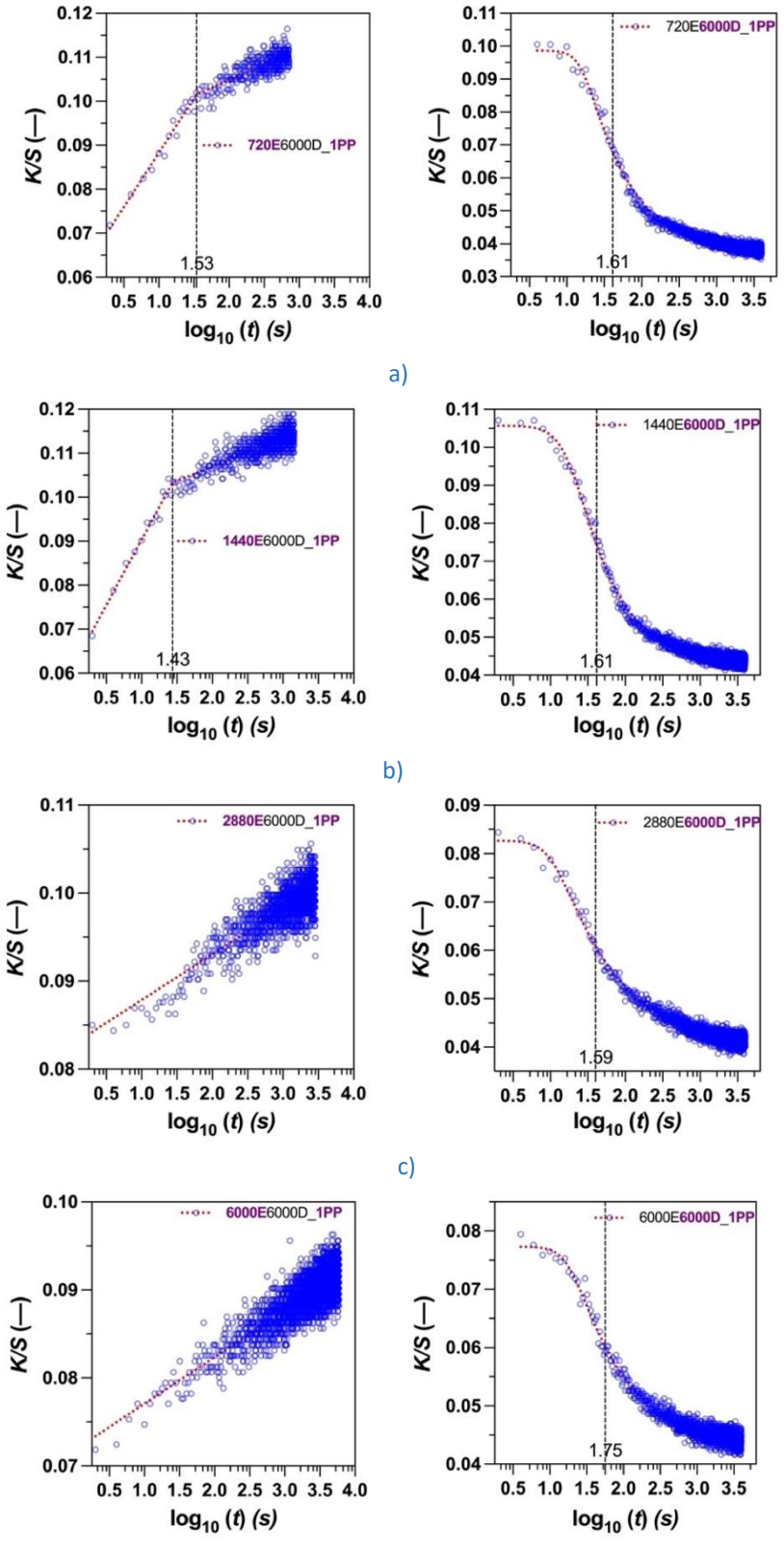

Figure 5.2. Experimental *K/S–time* data (blue) and best-fit curves (red, dotted) for growth and decay of photochromic nonwovens at 10 g·kg^{-1} under four irradiance protocols: (a) 720E6000D, (b) 1440E6000D, (c) 2880E6000D, (d) 6000E6000D

5.5.2 Thermal Fading (D) in low-loaded nonwovens: Asymmetric 5PL

Decay traces for low-loaded nonwovens are strongly **asymmetric in the log-time domain**: a fraction relaxes quickly, followed by a pronounced **long-tail** from slowly relaxing or partially stabilised populations. This behaviour is not captured reliably by simple exponentials or symmetric logistic models.

An **asymmetric 5-parameter logistic (5PL)** model provides the appropriate description, reproducing both the fast initial relaxation and the extended tail. The fitted **asymmetry parameter** deviates markedly from unity, confirming a skewed relaxation-time distribution; together with the **midpoint time**, it compactly quantifies the heterogeneous decay behaviour.

This asymmetry indicates relaxation pathways distributed across multiple microenvironments with different thermal accessibility and constraint (fibre–dye interactions, free-volume variations, and oxygen accessibility), supporting the need for **logistic (5PL)** rather than exponential modelling.

5.5.3 Unified Growth–Decay Interpretation in Low-Loaded Nonwovens

Taken together, low-loaded nonwovens show a kinetic signature fundamentally different from prints: **multi-regime exposure growth** coupled with **asymmetric, distributed (5PL) decay**, consistent with volumetric dye distribution and strong optical/microenvironmental heterogeneity.

Fatigue in these systems affects both **amplitude and shape**. With increasing cumulative UV dose, the balance between fast/slow exposure regimes shifts and decay becomes more asymmetric, indicating **selective photodegradation** of dye populations in different local environments. This demonstrates that apparent kinetics are governed by distributed pathways rather than a single dominant process.

Within the unified framework, regime-based exposure analysis, combined with asymmetric logistic decay modelling, captures this complexity in a controlled, comparable way and strengthens the architecture-discrimination basis for accepting **H3** when contrasted with the near-ideal print reference.

5.6 Kinetic Behaviour of High-Loaded Photochromic Nonwovens (50 g·kg^{-1})

Highly loaded photochromic nonwovens are volumetrically dyed porous architectures in which elevated dye concentration amplifies **optical screening (inner-filtering)**, **aggregation**, and **microenvironmental constraints**. UV penetration is therefore strongly reduced, producing excitation conditions—and kinetic signatures—distinct from both prints and low-loaded nonwovens.

5.6.1 Photocolouration (Exposure Phase): Constraint-Dominated Mono-Exponential Behaviour

Exposure traces appear **mono-regime** across protocols, with linearised diagnostics showing minimal curvature and supporting a single apparent growth descriptor. However, this apparent simplicity is not evidence of homogeneity (as in prints); it reflects **constraint-dominated excitation**. At high loading, UV is attenuated near the surface, so the measured $K/S_{(t)}$ response is dominated by a shallow, optically accessible subset of the dye population, while deeper populations contribute little—suppressing the slower components seen in low-loaded nonwovens.

With increasing cumulative UV dose, the apparent growth rate decreases steadily, indicating fatigue-driven suppression of effective photoconversion. This trend is consistent with **depletion/inactivation of the accessible photoactive population** rather than redistribution between kinetic regimes; thus, fatigue is expressed mainly as reduced **growth efficiency** rather than a change in regime structure.

Table 5.3. Best-fit parameters and goodness-of-fit statistics for the **growth (G)** phase (top) and **decay (D)** phase (bottom) corresponding to **Figure 5.3**.

Best-fit values	Growth phase: **720E**6000D_**5PP**	Growth phase: **1440E**6000D_**5PP**	Growth phase: **2880E**6000D_**5PP**	Growth phase: **6000E**6000D_**5PP**
Intercept a_1	0.2949	0.3058	0.2608	0.2092
Slope 1 b_1	0.06179	0.06135	0.05768	0.03135
R^2	0.9157	0.9214	0.9287	0.8839
Preferred model	**Linear Regression**	**Linear Regression**	**Linear Regression**	**Linear Regression**

Best-fit values	Decay phase: 720E**6000D_5PP**	Decay phase: 1440E**6000D_5PP**	Decay phase: 2880E**6000D_5PP**	Decay phase: 6000E**6000D_5PP**
Hillslope (η)	-2.594	-3.531	-2.892	-4.697
Skewness (α)	0.2224	0.1361	0.1372	0.06868
Top plateau $(K/S)_\infty$	0.3274	0.39	0.3524	0.2586
Bottom Plateau $(K/S)_0$	0.04904	0.05167	0.04695	0.03138
t_{50} (s)	41.82	50.97	70.32	120.4
R^2	0.9962	0.9975	0.9962	0.9941
Preferred model	**Sigmoidal (5PL)**	**Sigmoidal (5PL)**	**Sigmoidal (5PL)**	**Sigmoidal (5PL)**

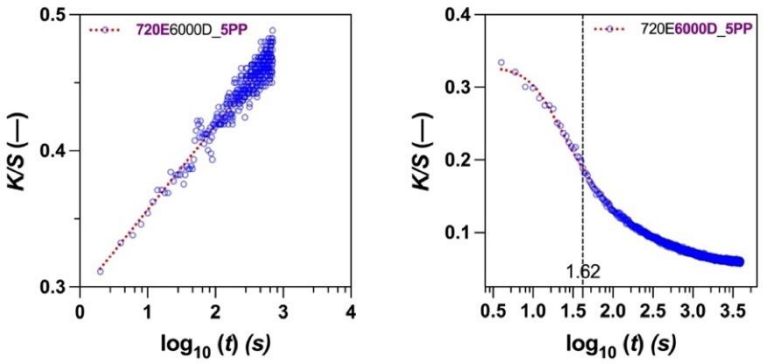

a)

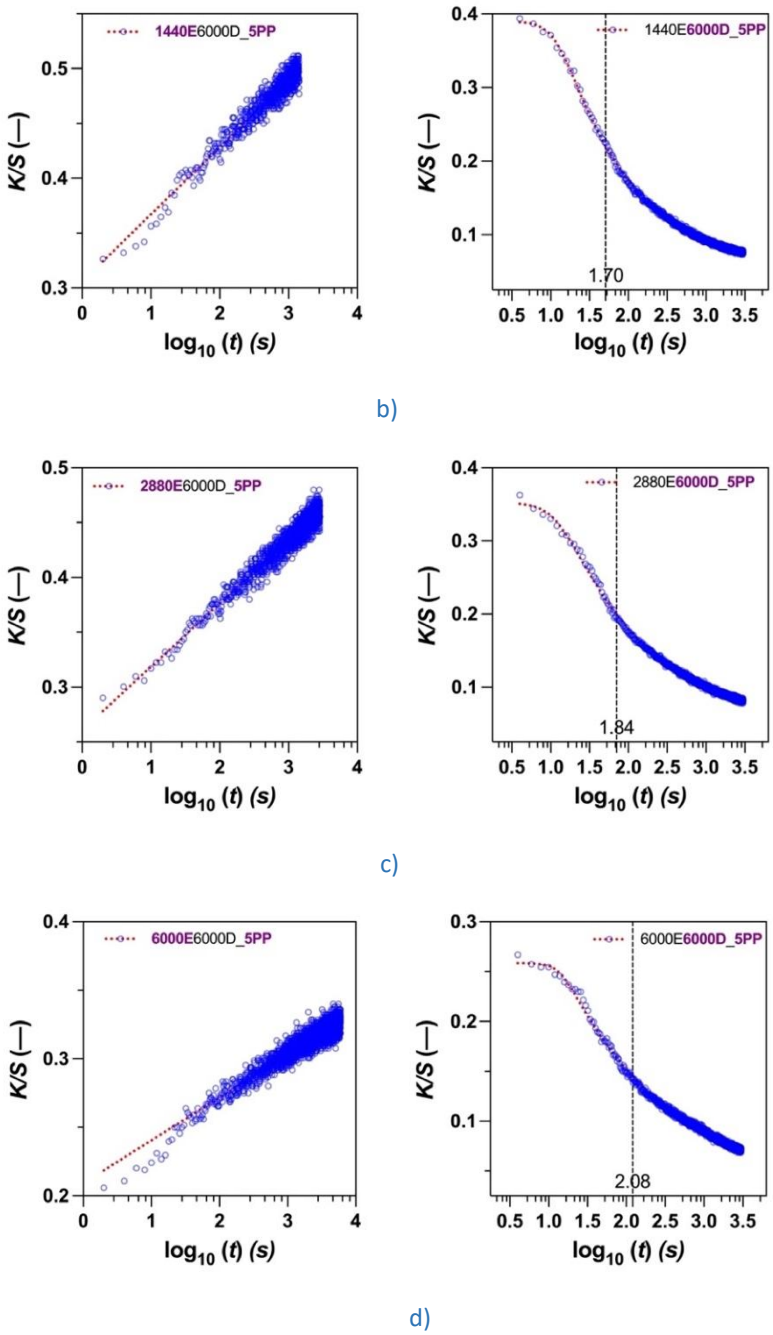

Figure 5.3. Experimental *K/S–time* data (blue) and best-fit curves (red, dotted) for growth and decay of photochromic nonwovens at 50 g·kg⁻¹ under four irradiance protocols**:** (a) 720E6000D, (b) 1440E6000D, (c) 2880E6000D, (d) 6000E6000D

5.6.2 Thermal Fading (D) in high-loaded nonwovens: Strongly Asymmetric 5PL

Highly loaded nonwovens exhibit the greatest departure from ideal decay behaviour. In the log-time domain, decay curves are **highly asymmetric**, with a delayed onset and an extended **slow tail**, which symmetric logistic or exponential models cannot represent without bias.

An **asymmetric 5PL** model fits the decay reliably, with asymmetry parameters far from unity. With increasing cumulative UV exposure, **midpoint times increase markedly**, indicating progressive slowing of dominant relaxation pathways. This

implies fatigue does more than reduce recoverable fraction—it **reshapes the relaxation-time distribution**.

The concurrent increase in midpoint time and asymmetry is consistent with the accumulation of **stabilised/trapped coloured populations** within the nonwoven. At high loading, aggregation, restricted mobility, and matrix interactions promote long-lived coloured states, and repeated UV exposure amplifies this heterogeneity.

5.6.3 Unified Growth–Decay Interpretation in High-Loaded Nonwovens

Considering exposure and decay together, high-loaded nonwovens exhibit a fatigue signature distinct from that of low-loaded systems. **Exposure** remains apparently mono-regime, but the **effective growth rate steadily decreases** with cumulative UV dose. **Decay** becomes progressively **slower and more asymmetric (5PL)**, indicating increasing dominance of constrained and partially non-reversible populations.

Thus, fatigue affects both phases: strong **optical screening** limits excitation from the outset, and repeated irradiation promotes accumulation of non-ideal populations that distort relaxation. The combined outcome is coupled suppression of **photocolouration efficiency** and **thermal recovery**.

Within the unified framework, high-loaded nonwovens illustrate how apparent kinetic simplicity can mask severe non-ideal behaviour; constraint-aware exposure analysis, together with asymmetric logistic decay modelling, provides robust, architecture-sensitive descriptors for cross-system comparison. Together with the print reference and low-loaded nonwovens, these results demonstrate systematic architecture/loading control of apparent kinetics and support acceptance of **H3**.

5.7 Architecture-Dependent Kinetic Discrimination and Validation of H3

Unified analysis of K/S–*time* profiles shows that **apparent kinetic descriptors reliably discriminate textile architectures**, even under identical dye chemistry and controlled irradiation. Prints and nonwovens display systematically different exposure and decay behaviour driven by differences in **optical coupling** and **microstructural constraint**.

- **Prints (surface-confined):** rapid, stable exposure growth (often captured by a single dominant regime) and **symmetric decay** well described by **4PL**. Fatigue appears mainly as **plateau/intensity loss** with limited shape distortion—yielding a near-ideal textile kinetic signature.
- **Low-loaded nonwovens (volumetric): multi-regime exposure** from depth-dependent activation and heterogeneous environments, and **asymmetric decay** requiring **5PL**. Fatigue shifts the balance of exposure regimes and increases decay asymmetry, consistent with **selective degradation** across microenvironments.
- **High-loaded nonwovens:** strong inner-filtering produces an apparently mono-regime exposure trace that is **constraint-dominated**; with cumulative UV dose, growth efficiency declines while decay becomes progressively **slower and more asymmetric (5PL)**, indicating coupled suppression of photocolouration and recovery.

Across systems, the combined descriptor set—exposure regime structure plus decay model family (**4PL vs 5PL**), characteristic times, and asymmetry—consistently distinguishes **prints vs nonwovens** and separates **low- vs high-loaded** volumetric systems. Because this discrimination follows from a unified, diagnostic-driven framework (rather than over-fitted mechanistic parameters), it provides robust cross-architecture comparability.

Therefore, Hypothesis H3 is accepted: the unified kinetic framework successfully discriminates textile architectures and captures systematic switching differences arising from dye distribution, optical screening, and microstructural heterogeneity, establishing a basis for subsequent dose-based photodegradation analysis.

6. Effect of Sustained UV Exposure on Dye Photodegradation

6.1 Concept of Cumulative UV Dose

While **Section 5** addresses reversible switching kinetics, practical photochromic textiles are ultimately limited by irreversible photodegradation under sustained or repeated UV exposure. A key difficulty is distinguishing true material degradation from protocol artefacts arising from differences in irradiance, exposure time, wavelength, and recovery structure. Reporting fatigue versus time or cycle count can be misleading because protocols with the same duration may deliver very different photon fluxes, and intermittent protocols (with recovery phases) are not directly comparable to continuous exposure.

To resolve this, the dissertation adopts cumulative UV dose as the primary independent variable, defined as the integrated UV energy delivered:

Cumulative UV dose and dose-based photofading:

$$H = E\,t;\; H = \sum_{i=1}^{n} E_i\,t_i$$

where, E_i and t_i correspond to irradiance and exposure time for the growth phase in the photohromic cycle.

Photodegradation is then quantified by tracking the dose-dependent decline in **exposure-phase intensity descriptors** (e.g., maximum/plateau or normalised plateau values) across cycles. This focuses the analysis on **irreversible loss of photoactive capacity**, rather than reversible changes in switching rate or relaxation shape.

Protocol structure still matters—because recovery phases can alter the recovery/fragmentation balance—but expressing degradation on a dose basis makes those effects explicit rather than confounded. This dose framework also supports comparison between monochromatic laboratory irradiation and broadband solar simulation once dose equivalence is defined, and it provides the basis for testing **H1 (cumulative-dose control of fatigue)** and **H2 (role of recovery phases)** in the sections that follow.

6.2 UV-Induced Fading in Photochromic Prints: Role of Time, Intensity, and Relaxation

Photochromic prints are an optically accessible, surface-confined architecture that minimises depth-dependent attenuation, making them a useful reference for isolating the effects of **exposure time, irradiance, and protocol structure** on UV-induced fatigue.

6.2.1 Time-Dependent Fading under Constant Irradiance

Under continuous UV at a fixed irradiance, prints show a monotonic decline in attainable colour intensity (e.g., maximum during exposure), consistent with cumulative, irreversible loss of photoactive dye. However, comparing fatigue at different irradiances reveals that **equal exposure times do not produce equal degradation**, demonstrating that time alone is not a reliable fatigue metric.

6.2.2 Intensity Effects and Dose Equivalence

When the same data are expressed as a function of **cumulative UV dose**, fading curves from different irradiances largely collapse onto a common trajectory. This indicates that, in prints, photodegradation is primarily governed by the **total delivered UV energy** rather than the specific time–irradiance combination. Small deviations at very high irradiance may reflect secondary effects (e.g., local heating), but the dose dependence remains dominant.

6.2.3 Influence of Relaxation Phases

Protocols that include relaxation periods (allowing partial thermal recovery) show **modestly slower fatigue** at the same cumulative dose, consistent with reduced accumulation of irreversible products. Conversely, suppressing relaxation (maintaining the coloured state longer) results in **slightly faster degradation**, suggesting a higher susceptibility of the merocyanine-rich state to irreversible pathways. In both cases, relaxation effects are **secondary** to cumulative dose.

6.2.4 Summary of Fading Behaviour in Photochromic Prints

- Exposure time alone does not reliably describe fatigue across irradiance levels.
- **Cumulative UV dose** provides a unifying degradation descriptor.
- **Relaxation phases** modulate the fatigue rate but do not change its fundamentally dose-driven nature.

6.3 Influence of Irradiation Wavelength (360 nm vs 380 nm)

UV wavelength affects both switching efficiency and degradation because absorption cross-section and photon energy vary with wavelength. Therefore, photodegradation was compared at **360 nm** and **380 nm** within the dose-based framework.

6.3.1 Switching Efficiency and Initial Intensity

At equal irradiance, **360 nm** produces a higher initial photocolouration efficiency than **380 nm**, resulting in a higher maximum during exposure, consistent with stronger activation. In prints, exposure-phase behaviour remains stable and reproducible at both wavelengths prior to significant fatigue, enabling controlled comparison of degradation trends.

6.3.2 Dose-based degradation trends

When degradation is plotted versus **cumulative UV dose**, the data at each wavelength show consistent dose dependence and collapse across irradiance levels onto **wavelength-specific dose–response curves**. For the same delivered dose, degradation proceeds **faster at 360 nm** than at 380 nm, consistent with higher photon energy and greater probability of irreversible side reactions at shorter wavelengths.

6.3.3 Implications for Dose-Based Comparability

The cumulative dose is a robust unifying metric **only within a fixed-wavelength context**. For cross-source comparisons (e.g., different UV lamps or solar simulation), dose equivalence must account for **spectral distribution**, not just total energy, or degradation severity can be systematically misestimated.

6.3.4 Summary (Wavelength Effects)

- Shorter wavelength (**360 nm**) accelerates degradation at a given dose.
- Dose-based collapse holds **within each wavelength**.
- Wavelength must be explicitly accounted for in fatigue assessment, supporting **H1** while defining its applicability limits.

6.4 Dye Concentration Effects in Photochromic Prints

Dye concentration controls both performance and fatigue in photochromic prints by changing optical density, excitation distribution, and the likelihood of intermolecular interactions. Evaluating concentration effects on a dose basis clarifies how fatigue develops even in a comparatively uniform, surface-confined architecture.

6.4.1 Initial Intensity and Optical Screening

Higher dye concentration increases the initial exposure-phase colour intensity (higher max K/S), but the increase is non-linear because **optical screening** increases at high loading. Stronger absorption confines the effective excitation closer to the surface, reducing the attainable intensity and increasing the local photon density, which can raise susceptibility to irreversible reactions.

6.4.2 Dose-based photodegradation

When plotted versus **cumulative UV dose**, higher-concentration prints show a **faster normalised decline** in colour intensity than lower-concentration prints. This indicates that increased loading, while improving initial colour strength, also increases fatigue per unit dose–consistent with enhanced dye–dye interactions, local heating, and higher fragmentation risk in densely populated merocyanine states. The trend remains after normalisation, confirming a real concentration effect rather than an artefact of higher absolute intensity.

6.4.3 Interaction with protocol structure

Protocol structure modulates the concentration effect: suppressing relaxation phases tends to amplify degradation in high-concentration prints at the same dose, consistent with prolonged residence in the coloured state. However, even with recovery periods, higher-concentration prints still degrade faster on a dose basis, showing concentration is an independent fatigue driver.

6.4.4 Summary of Concentration Effects in Prints

- Higher concentration increases initial intensity but increases **optical screening**.
- Fatigue accelerates with concentration when expressed as a function of **cumulative dose**.
- Concentration effects persist across protocol structures.

These results motivate extending dose-based fatigue analysis to volumetric nonwovens, where penetration depth and microenvironmental heterogeneity add further complexity.

6.5 Photodegradation in Photochromic Nonwovens: Concentration and Architectural

Photochromic nonwovens differ fundamentally from prints due to **volumetric dye distribution**, high porosity, strong scattering, and **depth-dependent UV attenuation**, producing heterogeneous excitation and degradation. As a result, dose-based analysis remains essential but requires architecture-aware interpretation.

6.5.1 Dose-Dependent Fading in Low-Loaded Nonwovens

Low-loaded nonwovens show a gradual decline in maximum attainable colour intensity with increasing **cumulative UV dose**. Dose-based plotting improves comparability across irradiances, but,unlike prints-curves do not fully collapse. This reflects **distributed excitation through thickness**: at low loading, UV penetrates deeply, and degradation is **non-uniform**, with surface-proximal regions degrading faster than deeper regions. As the balance of depth contributions shifts with dose, the apparent degradation rate evolves. Even so, cumulative dose remains a useful organising variable for the overall fatigue trend.

6.5.2 High-Loaded Nonwovens: Enhanced Optical Screening and Accelerated Fatigue

Highly loaded nonwovens exhibit strong **inner filtering**, confining excitation to a shallow surface region. Photodegradation therefore proceeds rapidly in the optically accessible zone, giving steep initial dose-response slopes (high fatigue susceptibility). The decline may later slow as readily excited populations are depleted and more constrained/shielded regions dominate the observable response. Despite a large total dye reservoir, strong screening can produce **rapid apparent fatigue** because deeper populations contribute little to the measured K/S.

6.5.3 Prints and Nonwovens (dose behaviour)

Prints typically show more uniform dose equivalence because dye is surface-confined and excitation is more uniform. Nonwovens show greater variability at the same cumulative dose because penetration depth, local environments, and the relative weighting of reversible/irreversible processes vary through thickness, especially at low loading.

6.5.4 Implications for Unified Fatigue Assessment

For nonwovens, cumulative UV dose is **necessary but not sufficient**: it captures the overall degradation progression, but architecture-specific optical and microenvironmental effects modulate the **rate and shape** of fatigue trajectories. This motivates combining the unified kinetic framework **(Section 5)** with dose-based

degradation analysis to interpret how reversible switching and irreversible fatigue interact in volumetric textile systems.

6.6 Protocol Mode Effects (A, B, C): Validation of H2

Photodegradation depends not only on the total UV dose but also on the **protocol structure**; specifically, how the dose is distributed over time and whether **recovery** is allowed between exposures. To test the **Recovery–Fragmentation Hypothesis (H2)**, fatigue was evaluated under three protocol modes that vary the extent of relaxation between UV steps.

6.6.1 Definition of Protocol Modes

- **Mode A (full recovery):** UV exposures are separated by long relaxation periods, allowing return close to baseline between cycles; minimises residence time in the coloured (merocyanine-rich) state.
- **Mode B (partial recovery):** shorter relaxation periods allow only partial return toward baseline; subsequent cycles begin from a partially coloured state.
- **Mode C (suppressed recovery):** relaxation is minimal/absent, keeping the system predominantly coloured across cycles; represents a worst-case condition for fatigue.

Together, Modes A, B and C provide a controlled way to probe the balance between **reversible recovery** and **irreversible fragmentation** pathways as protocol boundary conditions are tightened.

6.6.2 Effect of Protocol Structure on Photodegradation Trajectories

When degradation is expressed as a function of **cumulative UV dose**, clear protocol-mode effects are evident. **Mode A** shows the **slowest fatigue rate** in both prints and nonwovens: providing full relaxation between exposures promotes recovery and reduces accumulation of irreversible photoproducts, thereby mitigating dose-driven degradation.

Table 6.1. **Goodness-of-fit statistics for the effect of photocolouration and photodegradation under** Protocol Mode A **for photochromic** nonwovens**.**

a) Photocolouration	10 g.kg^{-1}	50 g.kg^{-1}
Equation	$K/S\,(-) = -0.00012\ H + 0.05$	$K/S\,(-) = -0.00052\ H + 0.32$
R^2	0.94	0.79
Sy.x	0.002	0.019

b) Photodegradation	10 g.kg^{-1}	50 g.kg^{-1}
Equation	$-(\log I - \log I_0)\,(-) = 0.00014\ H - 0.023$	$-(\log I - \log I_0)\,(-) = 0.00087\ H + 0.0074$
R^2	0.91	0.80
Sy.x	0.031	0.031

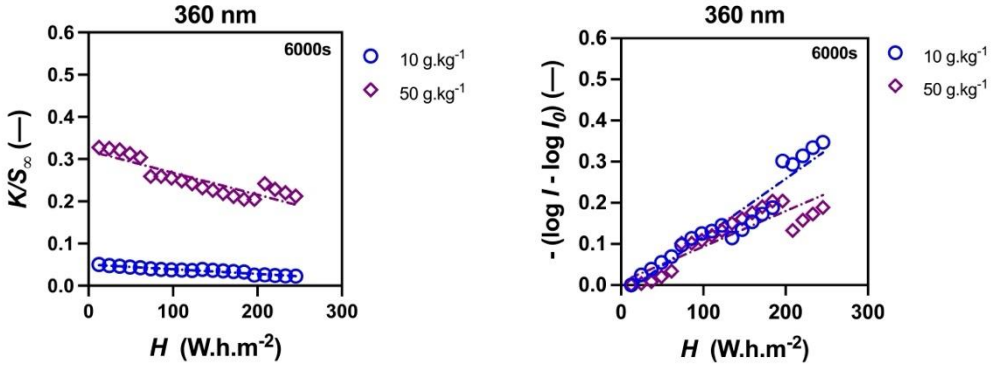

a) b)

Figure 6.1. Effect of photodegradation under Protocol Mode A for nonwovens: (a) Photocolouration response, (b) Photodegradation (fatigue)

Mode B shows intermediate fatigue behaviour. Partial relaxation slows degradation relative to near-continuous exposure, but recovery is incomplete, so irreversible damage still accumulates. Consequently, the dose–response curve consistently falls between Mode A (slowest) and Mode C (fastest**)** across the studied architectures.

Table 6.2. Goodness-of-fit statistics for the effect of photocolouration and photodegradation under Protocol Mode B

a) Photocolouration	2 g.kg^{-1}	8 g.kg^{-1}
Equation	$K/S\,(-) = -0.000511\,H + 0.1087$	$K/S\,(-) = -0.00113\,H + 0.4179$
R^2	0.93	0.95
Sy.x	0.00071	0.0012

b) Photodegradation	2 g.kg^{-1}	8 g.kg^{-1}
Equation	$-(\log I - \log I_0)\,(-) = 0.00210\,H + 0.0022$	$-(\log I - \log I_0)\,(-) = 0.001202\,H - 0.0023$
R^2	0.93	0.95
Sy.x	0.0028	0.0013

c) Photocolouration	100 g.kg^{-1}	200 g.kg^{-1}
Y_0	5.922	10.73
Plateau	4.82	7.64
k	0.3790	0.3941
H	2.639	2.537
Span	1.098	3.085
R^2	0.99	0.99
Sy.x	0.0177	0.0763
RMSE	0.0156	0.0673
AIC_c	−68.18	−39.01

d) Photodegradation	100 g.kg^{-1}	200 g.kg^{-1}
Y_0	−0.0145	−0.0229
Plateau	0.0753	0.1261
k	0.3551	0.3506
H	2.816	2.852
Span	0.0899	0.1491
R^2	0.99	0.99
Sy.x	0.00139	0.0036
RMSE	0.00122	0.00319
AIC_c	−119.1	−100.0

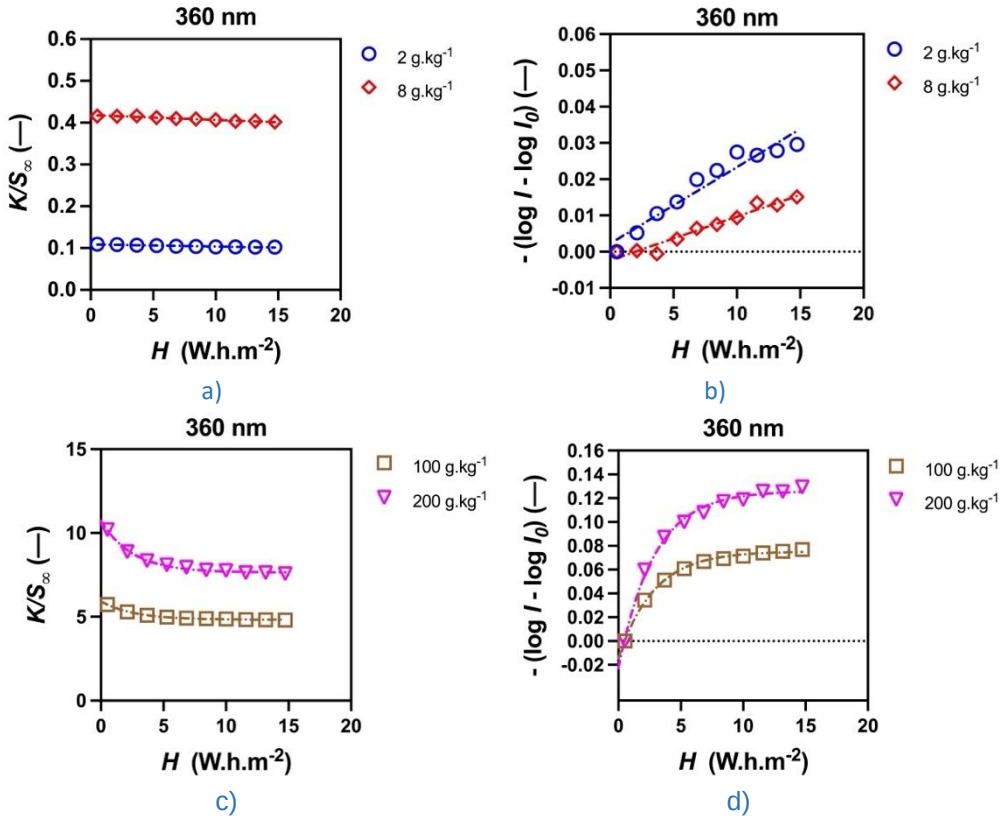

Figure 6.2. Effect of photocolouration and photodegradation under Protocol Mode B for photochromic prints with low and high dye content :
(a) photocolouration, (b) photodegradation, (c) photocolouration, (d) photodegradation

Mode C produces the **fastest degradation** at the same cumulative UV dose. With relaxation suppressed, the dye spends longer in the coloured (merocyanine-rich) state, increasing its susceptibility to irreversible fragmentation and accelerating fatigue. The effect is strongest in **highly loaded nonwovens**, where optical screening and microenvironmental constraints further stabilise the coloured state and amplify long-lived, degradation-prone populations.

Table 6.3. Goodness-of-fit statistics for the effect of photocolouration and photodegradation under Protocol Mode C

a) Photocolouration	2 g.kg^{-1}	8 g.kg^{-1}
Equation	$K/S\,(-) = -0.0006947\ H + 0.1119$	$K/S\,(-) = -0.003122\ H + 0.4088$
R^2	0.96	0.94
Sy.x	0.00065	0.0039

b) Photodegradation	2 g.kg^{-1}	8 g.kg^{-1}
Equation	$-(\log I - \log I_0)\,(-) = 0.002835\ H - 0.0018$	$-(\log I - \log I_0)\,(-) = 0.00349\ H + 0.00511$
R^2	0.96	0.94
Sy.x	0.0026	0.0041

c) Photocolouration	100 g.kg^{-1}	200 g.kg^{-1}
Y_0	5.99	12.64
Plateau	5.005	10.94
k	0.1563	0.2986
H	6.398	3.349
Span	0.9857	1.703
R^2	0.99	0.94
Sy.x	0.0095	0.1247
RMSE	0.0084	0.110
AIC_c	−80.54	−29.20

d) Photodegradation	100 g.kg^{-1}	200 g.kg^{-1}
Y_0	−0.00653	−0.01174
Plateau	0.07271	0.0519
k	0.1456	0.2927
H	6.867	3.417
Span	0.0792	0.0636
R^2	0.99	0.94
Sy.x	0.00083	0.0049
RMSE	0.00073	0.0043
AIC_c	−129.3	−93.89

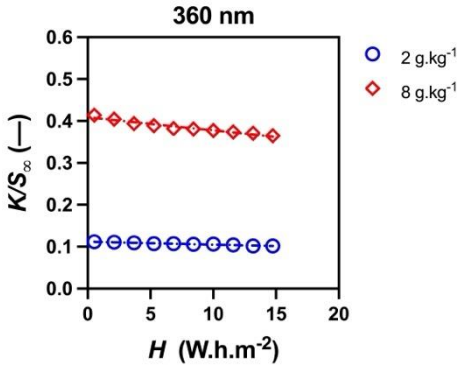

a)

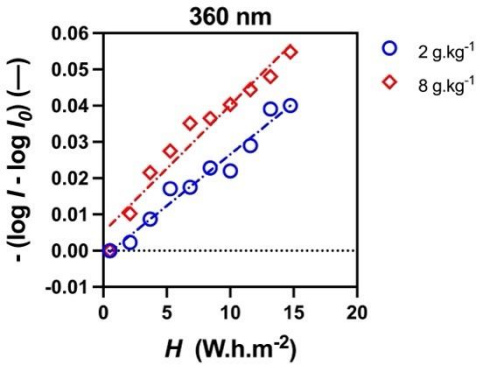

b)

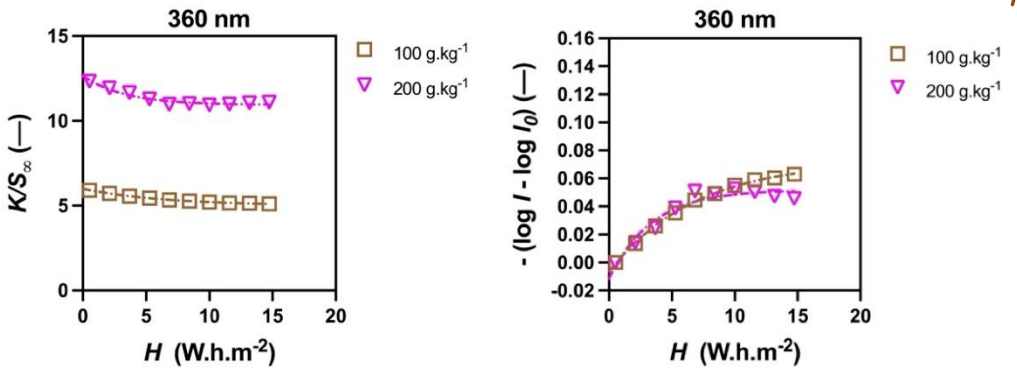

c) d)

Figure 6.3. Effect of photocolouration and photodegradation under Protocol Mode C for photochromic prints with low and high dye content**:** (a) Photocolouration, (b) Photodegradation, (c) Photocolouration, (d) Photodegradation

6.6.3 Architecture-Dependent Sensitivity to Protocol Effects

Protocol-mode separation is **architecture-dependent**. **Prints** show only modest differences between Modes A, B and C, consistent with near-ideal switching and efficient thermal recovery. **Nonwovens**, especially at **high dye loading**, are much more sensitive: restricted mobility and heterogeneous environments amplify the effect of prolonged activation, increasing susceptibility to degradation when relaxation is limited. This highlights the need for protocol-aware testing in volumetric systems; protocols that appear benign for prints can misrepresent durability in nonwovens or mask degradation mechanisms if recovery effects are not controlled.

6.6.4 Validation of H2

The consistent ordering **Mode A (slowest) < Mode B < Mode C (fastest)** at equivalent cumulative dose directly supports **H2**: relaxation promotes recovery and slows fatigue, while suppressing relaxation accelerates irreversible fragmentation. This does not contradict dose control; rather, **cumulative UV dose** sets the overall degradation potential, and **protocol structure** modulates how efficiently that dose is converted into irreversible damage. Therefore, **Hypothesis H2 is accepted**.

6.7 Accelerated Ageing and Solar Simulation (SUNTEST CPS+)

Monochromatic UV testing offers tight control of wavelength and protocol, but practical durability must also be assessed under **broadband, solar-like exposure**. To bridge laboratory UV studies and outdoor-relevant conditions, accelerated ageing was performed using a xenon solar simulator (**SUNTEST CPS+**).

6.7.1 Rationale for Solar Simulation Testing

Solar irradiation includes UV, visible, and infrared components that act together: **UV** drives photocolouration and degradation, **visible light** promotes bleaching, and **IR** elevates temperature, modifying relaxation kinetics. The SUNTEST experiments, therefore, evaluate whether degradation trends from controlled UV protocols remain interpretable when multiple spectral and thermal effects act simultaneously, and whether **dose-based concepts** retain qualitative value.

6.7.2 Degradation Behaviour under SUNTEST

Both prints and nonwovens show progressive loss of maximum attainable colour intensity, consistent with irreversible photodegradation. Architecture and concentration effects persist: prints degrade more gradually**,** whereas nonwovens—especially high-loaded—fatigue faster**.** Although exact spectral dose equivalence to monochromatic UV cannot be defined directly, the relative durability ranking observed under controlled UV remains consistent under SUNTEST exposure.

6.7.3 Thermal and Visible-Light Effects

Broadband exposure introduces continuous visible light and increased sample temperature. These factors can partially mitigate long-lived coloured-state accumulation by accelerating relaxation and promoting bleaching, reducing residence time in the activated state. However, irreversible degradation continues to progress steadily, indicating that recovery pathways cannot fully offset sustained photon flux under solar-simulated conditions.

6.7.4 Implications

SUNTEST results show the dissertation's unified framework remains **qualitatively valid** under complex irradiation: dose-based, architecture-aware descriptors developed under monochromatic UV provide reliable **screening and comparative guidance**. Quantitative lifetime prediction would require spectral weighting and environmental modelling, but the laboratory UV approach is defensible for ranking materials and identifying failure-prone architectures prior to field deployment.

Table 6.4. Goodness-of-fit statistics for photocolouration and photodegradation behaviour of dye in photochromic prints

a) Photocolouration	Without filter	With filter
Equation	$K/S\,(-) = -0.01764\,H + 9.644$	$K/S\,(-) = -0.006207\,H + 10.97$
R^2	0.89	0.95
Sy.x	0.5794	0.1202

b) Photodegradation	Without filter	With filter
Equation	$-(\log I - \log I_0)\,(-) = 0.00113\,H + 0.0266$	$-(\log I - \log I_0)\,(-) = 0.000262\,H - 0.0049$
R^2	0.95	0.93
Sy.x	0.0228	0.0062

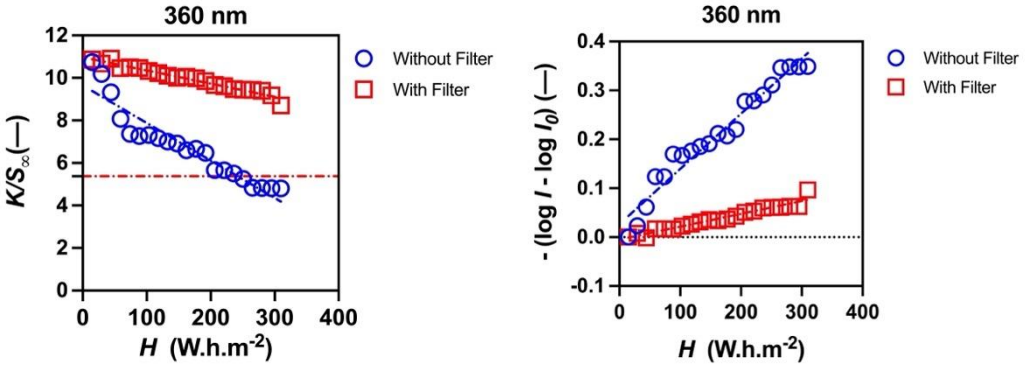

a) b)

Figure 6.4. SUNTEST CPS+ results for photochromic prints, showing the effect on (a) Photocolouration and (b) Photodegradation (fatigue)

6.8 Dose-Based Interpretation and Validation of H1

H1 is supported: irreversible photodegradation is governed primarily by **cumulative UV dose** (total delivered UV energy), rather than time, irradiance, or protocol structure considered alone, across the tested architectures, concentrations, wavelengths, and modes.

Prints: At fixed wavelength, degradation plotted vs dose shows strong consistency; data from different irradiances largely collapse onto a single dose–response curve. Protocol/relaxation effects change the *rate* slightly but do not override dose dependence.

Nonwovens: Dose remains the main organising variable, but architecture introduces deviations. Low-loaded systems show evolving apparent degradation as depth contributions shift with fatigue; high-loaded systems show rapid early loss dominated by the optically accessible region under strong screening. Curve collapse is therefore imperfect, yet overall trends remain dose-governed.

Wavelength: Shorter wavelengths (e.g., 360 nm) accelerate degradation at the same dose, but within a fixed wavelength, dose-based comparability holds.

SUNTEST: Under broadband solar simulation, exact spectral dose equivalence is not available, but relative durability rankings from controlled UV testing are preserved, consistent with cumulative energy input remaining dominant.

Overall, **dose is the primary driver**, while architecture, concentration, wavelength, and protocol structure **modulate the partitioning of dose between reversible recovery and irreversible damage**.

7. Discussion: Integrated interpretation of kinetics and fatigue

Sections 5 and 6 show that reversible switching kinetics and irreversible photodegradation in photochromic textiles are **coupled**, with the measured response shaped by optical transport, architecture, and protocol boundary conditions. Integrating unified kinetics with dose-based fatigue provides a coherent explanation of performance differences across systems.

7.1 Optical Coupling governs apparent kinetics

Apparent kinetics in textiles reflect **optical–photokinetic coupling** rather than intrinsic reaction rates alone, because diffuse reflectance–derived spectra embed absorption, scattering, and depth-dependent attenuation. In **prints**, coupling is comparatively weak (short path length, lower heterogeneity), so exposure and decay approach near-ideal behaviour and remain stable across cycles. In **nonwovens**, strong scattering and depth-dependent excitation produce **distributed exposure regimes** and **asymmetric decay**, which cannot be captured reliably by single-rate descriptors. The unified framework accommodates this by treating kinetic parameters as **conditional, operational descriptors**, avoiding mechanistic over-interpretation while preserving architectural discrimination.

7.2 Fatigue reshapes kinetics, not just intensity

Photodegradation reduces attainable colour intensity and can distort kinetic shape. In **nonwovens**, cumulative UV exposure selectively suppresses slower exposure regimes and increases decay asymmetry, indicating environment-dependent degradation of different dye populations. In **prints**, fatigue is mainly expressed as a plateau loss with limited change in kinetic shape. This contrast shows fatigue acts as an architecture-dependent restructuring of the effective kinetic landscape, supporting the need to analyse switching and degradation jointly.

7.3 Protocol structure modulates pathways (secondary to dose)

Protocol mode studies demonstrate that relaxation phases reduce degradation rate by decreasing time spent in the coloured (merocyanine-rich) state and limiting fragmentation pathways. However, recovery cannot eliminate fatigue: degradation still progresses monotonically with cumulative UV dose. In practice, recovery-friendly protocols can extend functional lifetime, but they do not replace material-level improvements in photostability; conversely, relaxation suppression can accelerate failure and amplify architectural differences.

7.4 Implications for textile design and evaluation

Surface-confined architectures provide **more stable kinetics and better fatigue resistance** under comparable conditions. Volumetric dye incorporation increases dye reservoir but introduces optical screening and heterogeneous degradation pathways that reduce durability. The unified kinetic + dose-based framework developed here enables realistic evaluation of these trade-offs using architecture-aware operational descriptors, supporting robust material screening, protocol design, and application-relevant performance assessment.

8. Conclusions and Contributions

8.1 Conclusions

- A unified kinetic and fatigue framework was established for evaluating photochromic textiles by analysing **K/S data in the log-time domain**, enabling consistent comparison across architectures and dye loadings.
- Photochromic response is strongly architecture-dependent**:** **prints** show near-**planar**, stable switching with first-order association behaviour, whereas **nonwovens** exhibit **porous/bulk constraints**, dose-sensitive multi-regime colouration, and asymmetric decay.
- **Bleaching kinetics** are consistently described by **logistic relaxation**, with **4PL** characterising **planar** print behaviour and **5PL** capturing nonwoven long-tail asymmetry associated with **constrained dye environments**.
- **Cumulative UV dose (irradiance × time)** is the primary driver of **irreversible photodegradation**, while wavelength, architecture, and protocol structure act as secondary modulators.
- Measurement **protocol design** influences apparent fatigue; continuous-irradiation approaches provide more reliable photofading assessment than interruption-heavy protocols.
- Performance trends are further influenced by **oxidation**, **temperature** (for T-type dyes), and **dispersion/processing quality**, especially in electrospun nonwovens.

8.2 Contributions

- Developed a **unified, diagnostic kinetic framework** for photochromic textiles using **KM-transformed versus log-time analysis** to extract operational kinetic descriptors across scattering substrates.
- Established **architecture-discriminating kinetic signatures**, including first-order association during colouration and **logistic (4PL/5PL)** decay during bleaching, with clear differentiation between prints and nonwovens.
- Demonstrated **UV-dose-based fatigue assessment** as a unifying method to compare degradation across irradiance levels (within wavelength-specific contexts).
- Quantified **protocol-dependent recovery/fragmentation effects** on fatigue curves and identified preferred measurement modes for robust photofading evaluation.
- Linked kinetic/fatigue behaviour to **formulation and manufacturing route** (dispersion, aggregation, bead formation) and supported interpretation using **FTIR, confocal Raman, and XRD**.

8.3 Hypotheses evaluation

1. **H1 (Cumulative UV Dose Hypothesis): Accepted.** Irreversible photodegradation is governed primarily by **cumulative UV dose (irradiance × time)**, while **wavelength, textile architecture, and protocol structure** act as secondary modulators.
2. **H2 (Recovery–Fragmentation Hypothesis): Accepted.** The presence or suppression of **recovery/relaxation phases** influences the balance between reversible recovery and irreversible fragmentation, thereby modulating the **rate and apparent trajectory of fatigue**.

3. **H3 (Unified Kinetics and Architecture Discrimination Hypothesis): Accepted.**
   Unified kinetic descriptors extracted from **K/S–time profiles** reliably discriminate textile architectures and capture systematic differences in switching and decay behaviour (e.g., **first-order association in colouration** and **logistic relaxation in bleaching**).

8.4 Scientific and Practical Significance

- **Scientific significance:** Provides a disciplined, architecture-aware framework for interpreting photochromic switching and fatigue in **heterogeneous, scattering textile media**, linking observed kinetics (growth/decay shape) to **microstructural constraints** and enabling comparable analysis across systems via **dose-based normalisation**.
- **Practical significance:** Delivers an actionable methodology for **material screening, protocol selection, durability testing, and lifetime prediction** of photochromic textiles/smart coatings, with clear guidance on how **architecture, UV dose, and testing protocol** influence performance and degradation.

9. Proposal for Further Research

1. **Isolate oxidation effects:** Use controlled-atmosphere validation (inert gas **N_2/Ar**) to separate oxygen-driven degradation from intrinsic switching and clarify oxidation-related fatigue/long-tail bleaching (especially in nonwovens).
2. **Extend DoE to performance mapping:** Build **architecture–dose–loading** performance maps (prints vs nonwovens) linking UV dose and dye loading to colour depth, switching rate, reversibility, and degradation, including identifying **threshold UV doses** for reproducible switching and stable parameter extraction.
3. **Generalise across chemistries/formulations:** Apply the unified framework (transformed ***Kubelka–Munk* / log-time** approach) to other photochromic systems to determine when **1–2 phase first-order association** is sufficient and when **logistic bleaching** is required, including transferability of **4PL (planar) vs 5PL (porous/bulk)** behaviour.
4. **Optimise electrospun systems:** Improve dispersion and electrospinning parameters to reduce aggregation and bead formation; quantify benefits via kinetic improvements (reduced asymmetry/tailing) and **lower UV dose** needed for measurable switching.
5. **Validate durability under field-relevant conditions:** Run long-term fatigue under **natural sunlight** with controlled environmental variables (humidity, temperature, oxygen level) to validate acceleration protocols and enable credible lifetime forecasting.

10 References

1. Dürr H, Bouas–Laurent H, editors. Photochromism: Molecules and Systems. Amsterdam: Elsevier; 2003.
2. Vik M, Periyasamy AP. Chromic Materials: Fundamentals, Measurements, and Applications. Boca Raton: CRC Press; 2018.
3. Periyasamy AP, Vikova M, Vik M. A review of photochromism in textiles and its measurement. Textile Progress. 2017;49(2):53–136. https://doi.org/10.1080/00405167.2017.1305833
4. Ramlow H, Andrade KL, Immich APS. Smart textiles: an overview of recent progress on chromic textiles. J Text Inst. 2021;112(1):152–171. https://doi.org/10.1080/00405000.2020.1785071
5. Bouas–Laurent H, Dürr H. Organic photochromism (IUPAC technical report). Pure Appl Chem. 2001;73(4):639–665. https://doi.org/10.1351/pac200173040639
6. Vikova M. Photochromic Textiles [doctoral dissertation]. Heriot–Watt University; 2011. http://hdl.handle.net/10399/2439
7. Little AF, Christie RM. Textile applications of photochromic dyes. Part 2: factors affecting the photocolouration of textiles screen–printed with commercial photochromic dyes. Colour Technol. 2010;126(3):164–170. https://doi.org/10.1111/j.1478–4408.2010.00242.x
8. Little AF, Christie RM. Textile applications of photochromic dyes. Part 3: factors affecting the technical performance of textiles screen–printed with commercial photochromic dyes. Colour Technol. 2011;127(5):275–281. https://doi.org/10.1111/j.1478–4408.2011.00307.x
9. Seipel S, Yu J, Periyasamy AP, Viková M, Vik M, Nierstrasz VA. Inkjet printing and UV–LED curing of photochromic dyes for functional and smart textile applications. RSC Adv. 2018;8(50):28395–28404. https://doi.org/10.1039/C8RA05856C
10. Solanki U, Viková M. Fatigue study of spiro[indoline–napthooxazines] pigment using colourimetric data in a continuous mode of UV irradiance. Fibres Textiles (Vlákna a textil). 2021;28(4):93–101. http://vat.ft.tul.cz/2021/4/VaT_2021_4_13.pdf
11. Solanki UB, Viková M, Holec P, Erben J, Vik M. Characterisation and photo–fatigue behaviour of UV–sensitive photochromic systems produced using electrospinning. J Ind Text. 2024;54:15280837241260068. https://doi.org/10.1177/15280837241260068
12. Viková M, Christie RM, Vik M. A unique device for measurement of photochromic textiles. Res J Text Appar. 2014;18(1):6–14. https://doi.org/10.1108/RJTA–18–01–2014–B002
13. Myrick ML, Simcock MN, Baranowski M, Brooke H, Morgan SL, McCutcheon JN. The Kubelka–Munk diffuse reflectance formula revisited. Appl Spectrosc Rev. 2011;46(2):140–165. https://doi.org/10.1080/05704928.2010.537004
14. Oleari C. Standard Colourimetry: Definitions, Algorithms and Software. Wiley; 2016.
15. Pimienta V, Lavabre D, Levy G, Samat A, Guglielmetti R, Micheau JC. Kinetic analysis of photochromic systems under continuous irradiation. Application to spiropyrans. J Phys Chem. 1996;100(11):4485–4490. https://doi.org/10.1021/jp9531117
16. Pimienta V, Micheau JC. Kinetic analysis of photoreversible photochromic systems under continuous monochromatic irradiation from Abs. vs time curves. Mol Cryst Liq Cryst A. 2000;344(1):157–162. https://doi.org/10.1080/10587250008023830
17. Pimienta V, Frouté C, Deniel MH, Lavabre D, Guglielmetti R, Micheau JC. Kinetic modelling of the photochromism and photodegradation of a spiro[indoline–naphthoxazine]. J Photochem Photobiol A. 1999;122(3):199–204. https://doi.org/10.1016/S1010–6030(99)00023–4
18. Maafi M. Useful spectrokinetic methods for the investigation of photochromic and thermo–photochromic spiropyrans. Molecules. 2008;13(9):2260–2302. https://doi.org/10.3390/molecules13092260
19. Delbaere S, Vermeersch G, Micheau JC. Quantitative analysis of the dynamic behaviour of photochromic systems. J Photochem Photobiol C. 2011;12(2):74–105. https://doi.org/10.1016/j.jphotochemrev.2011.05.004
20. Mohn E. Kinetic characteristics of a solid photochromic film. Appl Opt. 1973;12(7):1570–1576. https://doi.org/10.1364/AO.12.001570
21. Bär R, Gauglitz G. Limitations to the kinetic analysis of thermoreversible photoreactions of photochromic systems. J Photochem Photobiol A. 1989;46(1):15–26. https://doi.org/10.1016/1010–6030(89)87029–7
22. Krongauz VA. Environmental effects on organic photochromic systems. In: Dürr H, Bouas–Laurent H, editors. Photochromism: Molecules and Systems. Elsevier; 2003. p. 793–821.
23. Baillet G, Giusti G, Guglielmetti R. Comparative photodegradation study between spiro[indoline–oxazine] and spiro[indoline–pyran] derivatives in solution. J Photochem Photobiol A. 1993;70(2):157–161. https://doi.org/10.1010–6030(93)85036–8
24. Salemi–Delvaux C, Luccioni–Houze B, Baillet G, Giusti G, Guglielmetti R. Effect of photodegradation on the thermal bleaching rate constant of photochromic compounds in spiro[indoline–pyran] and spiro[indoline–oxazine] series. J Photochem Photobiol A. 1995;91(3):223–232. https://doi.org/10.1016/1010–6030(95)04113–X
25. Pariani G, Quintavalla M, Colella L, et al. New insight into the fatigue resistance of photochromic 1,2–diarylethenes. J Phys Chem C. 2017;121(42):23592–23598. https://doi.org/10.1021/acs.jpcc.7b04848
26. Salemi–Delvaux C, Pottier E, Guglielmetti R, Dubest R, Aubard J. Fatigue resistance of photochromic 2,2–diaryl–[2H]–heteroannellated chromenes in solution. Dyes Pigments. 1999;40(2–3):157–162. https://doi.org/10.1016/S0143–7208(98)00043–6
27. Yalcinkaya F. Preparation of various nanofiber layers using wire electrospinning system. Arab J Chem. 2019;12(8):5162–5172. https://doi.org/10.1016/j.arabjc.2016.12.012
28. Khatri Z, Ali S, Khatri I, Mayakrishnan G, Kim SH, Kim IS. UV–responsive polyvinyl alcohol nanofibers prepared by electrospinning. Appl Surf Sci. 2015;342:64–68. https://doi.org/10.1016/j.apsusc.2015.03.046
29. Doan HN, Tsuchida H, Iwata T, et al. Fabrication and photochromic properties of Forcespinning® fibers based on spiropyran–doped PMMA. RSC Adv. 2017;7(53):33061–33067. https://doi.org/10.1039/C7RA03794E

List of publications

1. **Solanki, U.**; Viková, M. "Fatigue Study of Spiro[Indoline–Napthoooxazines] Pigment Using Colourimetric Data in a Continuous Mode of UV Irradiance." *Fibres and Textiles*, 28(4), 2021, pp. 1–9. http://vat.ft.tul.cz/2021/4/VaT_2021_4_13.pdf
2. Viková, M.; **Solanki, U.**; Vik, M. "New Method for Prediction of Photochromic Textiles Fatigue Behaviour." *Materials Science Forum*, Vol. 1063, 2022, pp. 163–172. DOI: https://doi.org/10.4028/p–ld65c6
3. **Solanki, U.**; Viková, M.; Holec, P.; Erben, J.; Vik, M. "Fabrication of UV–Responsive Chromic System Using Nanospider Device and its Photo–Fatigue Behaviour Under Continuous Mode of UV Irradiance." In: *AUTEX 2022 Conference Proceedings*, Łódź, Poland, 2022. https://doi.org/10.34658/9788366741751.99
4. **Solanki, U. B.**; Viková, M.; Holec, P.; Erben, J.; Vik, M. "Characterisation and photo–fatigue behaviour of UV–sensitive photochromic systems produced using electrospinning." *Journal of Industrial Textiles*, Vol. 54, 2024, pp. 1–18. https://doi.org/10.1177/15280837241260068
5. **Solanki, U. B.**; Vikova, M.; Vik, M. "Spectrokinetic Investigation of the Photochromic System Under Continuous UV Irradiance Using Reflectance vs. Time Curves." *Fibres and Textiles*, 31(2), 2024, pp. 35–41. DOI: https://doi.org/10.15240/tul/008/2024–2–005
6. **Solanki, U. B.**; Viková, M.; Vik, M. "Photochromic Print's Distinct Photo–Fading Characteristics under Continuous UV Irradiation Measurement Modes." *Fibres & Textiles in Eastern Europe*, 33(1), 2025, pp. 87–95. DOI: https://doi.org/10.2478/ftee–2025–0009
7. **Solanki, U. B.**; Viková, M.; Vik, M "Transferable kinetic descriptors for photochromic colouration and thermal fading in photochromic textiles: surface-dyed versus bulk-dyed architectures. " **RSC Advances (Manuscript Submitted)**

Contribution to Conference Proceedings

1. **Solanki, U.,** Viková, M., Vik, M. *New method for prediction of photochromic textiles fatigue behaviour.* Poster presentation in Autex 2021 conference, 6–8 September, Guimares, Portugal,2021. (Online mode – Oral presentation)
2. **Solanki, U.,** Viková, M., Holec, P., Erben, J., Vik, M. *Fabrication of UV–responsive chromic system using nanospider device and its photo–fatigue behaviour under continuous mode of UV irradiance*, AUTEX 2022 Conference 9th June, LODZ, Poland,2022 (Online mode – Oral presentation)
3. **Solanki U.,** Viková M., Holec P., Erben J. *Fabrication of photochromic nanofibers with enhanced lightfastness by in–mold dyeing.* Poster presentation in Textile Research symposium '49 (TRS49) Conference, 8–10 October, Kyoto, Japan,2022, (Online mode). (Extended Abstract and Poster presentation).
4. **Solanki U.,** A R Tehrani–Bagha, Viková M., *Cotton fabrics cationisation and reactive dyeing*, Material Research and sustainable society symposium, 7th June, 2023, Liberec (Offline mode – Oral presentation).
5. **Solanki, U.,** Viková, M., and Vik, M. *Photo–fatigue behaviour of photochromic prints using continuous UV irradiance modes.* Poster presentation in Autex 2024 conference, 17–19 June, Liberec, Czech Republic, 2024. (Offline mode) (Poster presentation, Extended abstract and Research article)

Citations

Utkarshsinh B. Solanki

Doctor of Philosophy · Fellow at Technical University of Liberec

Liberec, Czechia

99 Influencing Photodegradation Parameters of Photochromic Dye's (photo merocyanine) form under continuous UV irradiance

10.7 Research Interest Score | **11** Citations | **2** h-index

Curriculum Vitae (CV)

Ing. Utkarshsinh Bhupendrasinh Solanki

Ph.D. Researcher (Materials Engineering) | Functional Photochromic Materials and UV–Responsive Textiles
Department of Material Engineering, Faculty of Textile, Technical University of Liberec (TUL), Liberec, Czech Republic
Email: utkarshsolanki78@icloud.com | ORCID: 0000–0003–0679–2443

RESEARCH PROFILE

Materials engineer and doctoral researcher focusing on photochromic systems for UV sensing and durable functional textiles. Experience spans the electrospinning of UV–responsive nanofibers (commercial Nanospider), spectrokinetic and colourimetric measurement protocols, multi–factorial kinetic modelling of photofading, and systematic evaluation of photodegradation drivers. Strong track record in protocol development, data analysis, and translating fundamental material behaviour into application–relevant performance metrics.
https://www.researchgate.net/profile/Utkarshsinh–Solanki

RESEARCH INTERESTS

Photochromic dyes and pigments; UV sensing and dosimetry; electrospun nanofibers; photodegradation and durability; colour science and colourimetry; optical spectroscopy (UV–Vis, reflectance); kinetic modelling; functional and smart textiles.

EDUCATION

Ph.D., Material Engineering, Technical University of Liberec (Czech Republic) 2019 – Present
Dissertation: **Factors affecting the measurements of photochromic materials**
Supervisor: **doc. Ing. Martina Viková, Ph.D.**
M.E., Textile Engineering, The Maharaja Sayajirao University of Baroda (India) 2015 – 2017
Thesis: Spunlace wound dressing with natural finish | GPA: 3.91/4.0
B.E., Textile Engineering, The Maharaja Sayajirao University of Baroda (India) 2011 – 2015 (GPA: 3.48/4.0)

RESEARCH AND PROFESSIONAL EXPERIENCE

Ph.D. Researcher, Technical University of Liberec (TUL), Czech Republic 2nd Oct 2019 – Present

- Investigate the kinetic and photo–fading behaviour of photochromic dyes/pigments under designed UV irradiance modes.
- Develop measurement protocols and quantitative techniques for spectro–kinetic and colourimetric analysis of photochromic systems.
- Model photo–fading characteristic curves under continuous UV irradiance; analyze fading kinetics using multi–factorial degradation models.
- Identify the key environmental and material parameters that influence photodegradation and photo–fatigue performance.
- Fabricate UV–responsive chromic systems and electrospun nanofibrous materials (Nanospider); evaluate durability and lightfastness.
- Apply materials characterisation methods, including UV–Vis/reflectance, FTIR, SEM, Raman microscopy, and colourimetry.

Junior Research Fellow (JRF), IIT Delhi (UAY Scheme) and Vardhman , India
2017 – 2019

*Project**: Detection of non–uniformity in fabrics (real–time)***

- Conducted applied research in textile chemistry and real–time detection of non–uniformity in dyed fabrics.
- Designed and developed a fabric defect detection system (FDDS) and detection algorithms using MATLAB (image processing).
- Contributed to the development of wound dressing materials with natural bio–finishes.

FUNDED PROJECTS AND LEADERSHIP

- Project leader: **Influence of chromic fabric preparation technology on fastness properties**, **SGS–2022–6039**, of the Technical University of Liberec, Czech Republic.
- Team member: **Colour appearance of products under different light sources**, **SGS–2020–6038** of the Technical University of Liberec, Czech Republic.
- Team member: **Enhancing pedestrian visibility in complex visual scenes in daytime and nighttime traffic conditions**, **SGS–2023–6385** of the Technical University of Liberec, Czech Republic.
- Team member of the project entitled "**Model pro predikci spektrálních vlastností textilii"** with grant number **SGS-2025-6565** of the Technical University of Liberec, Czech Republic.
- Junior researcher fellow (JRF): Detection of Non-Uniformity in Dyed Textile Materials using Image Analysis (**RP03290**) (IIT Delhi, India).

AWARDS AND ACHIEVEMENTS

- **Junior Research Fellowship (JRF)**, funded by MHRD and Ministry of Textiles (India), 2017–2019.
- **GATE** Qualified (2015), All India Rank (AIR) **94**.
- **Best presentation award:** Influence of chromic fabric preparation technology on fastness properties (SGS–2022–6039).
- **First Class with Distinction** in B.E. and M.E. degrees.

TECHNICAL SKILLS

- **Characterisation and measurement:** UV–Vis/reflectance, FTIR, SEM, Raman microscopy, colourimetry, viscosity measurement, particle size analysis.
- **Processing and fabrication:** electrospinning (commercial Nanospider), screen printing; fabrication of UV–responsive chromic systems.
- **Data analysis and modelling:** kinetic modelling; designed experiments (DoE); GraphPad Prism; MATLAB (image processing, neural networks, basic scripting); numerical analysis (basic C++).
- **Design tools:** AutoCAD; CREO 2.0; ChemDraw.

LANGUAGES

Hindi and Gujarati (native); English (fluent); Sanskrit; Czech (A2); German (A2).

RESEARCH VISITS AND INTERNSHIPS

- **Aalto University**, Espoo, Finland (research visit/internship).
- **Indian Institute of Technology Delhi (IIT Delhi),** New Delhi, India (research internship/association).

REFERENCES

- **doc. Ing. Martina Viková, Ph.D.**, Associate Professor, Department of Material Engineering, Faculty of Textile, Technical University of Liberec (TUL) | martina.vikova@tul.cz
- **Prof. M. Vik, Ph.D.**, Professor, Department of Material Engineering, Faculty of Textile, Technical University of Liberec (TUL) | michal.vik@tul.cz
- **Prof. Samrat Mukhopadhyay, Ph.D.**, Professor, Department of Textile and Fibre Engineering, Indian Institute of Technology Delhi (IIT Delhi) | samrat@textile.iitd.ac.in

Brief description of the current expertise, research and scientific activities

Name	**Ing. Solanki Utkarshsinh Bhupendrasinh (T19000375)**
Doctoral studies	**Textile Technics and Materials Engineering (P0723D270003)**
Study Mode	**Full–time**
Course Exams	1. Structure and properties of textile fibre (KMI/D136) Date: 13–12–2019 Status: **Completed**
	2. Mathematical Statistics (KAP/D126) Date: 04–06–2020 Status: **Completed**
	3. Optics of Solids (KMI/D118) Date: 04–02–2021 Status: **Completed**
	4. Experimental technique of the textile (DFT/D33) Date: 24–11–2023 Status: **Completed**
	5. Sensorical Textile Materials (KMI/D119) Date: 11–01–2024 Status: **Completed**
SDE exam	**PASS on 12.02.2025 (Status: Completed)**
Research projects	1. Team member of the project entitled **Colour appearance of products under different light sources** with grant number **SGS–2020–6038** of Technical University of Liberec, Czech Republic. 2. Project leader of the project entitled **Influence of chromic fabric preparation technology on fastness properties** with grant number **SGS–2022–6039** of Technical University of Liberec, Czech Republic 3. Team member of the project entitled **Enhancing pedestrian visibility in complex visual scenes in daytime and nighttime traffic conditions** with grant number **SGS–2023–6385** of Technical University of Liberec, Czech Republic. 4. Team member of the project entitled **Model pro predikci spektrálních vlastnosti textilii** with grant number **SGS-2025-6565** of Technical University of Liberec, Czech Republic.
Internships	1. Aalto University, Finland.
	2. Indian Institute of Technology, Delhi, India.
Award	Best Oral presentation Award for **Influence of chromic fabric preparation technology on fastness properties (SGS–2022–6039)**

Recommendation of the supervisor

Opinion of the supervisor on Ph.D. thesis Utkarshsinh Bhupendrasinh Solanki, M.E.

This dissertation focuses on the photokinetics and photodegradation of textile-based photochromic systems and represents a significant and original contribution to the field of advanced functional materials.

Mr. Solanki addresses a well-recognized limitation in the practical implementation of photochromic materials: their limited lightfastness and performance degradation under repeated UV activation. Through his systematic investigation of surface-applied and mass-dyed textile systems that incorporate a spiroxazine-based dye, Mr. Solanki has demonstrated strong experimental capability and a deep understanding of material behavior in real-world conditions.

One of the most impressive aspects of this work is the development of a rigorous, response-based methodology for quantifying photofading and photofatigue in solid-state systems. The lack of standardized evaluation protocols has long hindered progress in this area. Mr. Solanki's approach provides a reproducible, analytically robust framework that can be broadly adopted by the research community and industry.

Their work further distinguishes itself through the integration of advanced kinetic modeling. They applied both linear and nonlinear regression techniques, including mono- and bi-exponential first-order kinetics, as well as four- and five-parameter logistic models. Mr. Solanki successfully characterized the dynamic processes governing photo-coloration and thermal fading. This dual-phase analytical strategy reflects a high level of intellectual maturity and methodological sophistication.

Importantly, the dissertation is not purely theoretical. The findings clearly demonstrate how substrate architecture, irradiation conditions, and environmental parameters influence degradation pathways and performance stability.

This makes the research highly relevant to the design and optimization of durable photochromic textiles, especially for applications like UV sensing and smart materials.

Throughout his doctoral studies, Mr. Solanki has demonstrated exceptional independence, critical thinking, and persistence. His ability to bridge experimental work with theoretical modeling while maintaining clarity and rigor in data interpretation is commendable. They have also demonstrated excellent communication skills, presenting complex concepts in a structured and accessible manner.

In summary, the candidate is an exceptional researcher with the technical expertise, creativity, and determination necessary for advanced scientific work. I am confident that they will contribute valuable insights to academia and industry, and I wholeheartedly recommend them.

In Liberec 22 April 2026 Assoc. Prof. Martina Viková, Ph.D.

Opponent's reviews

Review to the dissertation titled with
"Factors affecting the measurements of Photochromic materials"

Photochromism is one of the most intriguing fields of photochemistry and has attracted considerable scientific and technological interest due to its broad range of applications, including UV sensing, smart textiles, optical data storage, adaptive coatings, and visual indicators. The incorporation of photochromic systems into textile substrates has further intensified this interest, while simultaneously introducing significant challenges related to measurement, durability, and reproducibility in optically complex fibrous media.

This doctoral thesis represents a high-quality, systematic, and methodologically rigorous contribution to photochromic textiles and functional colour measurement. It addresses the critical challenge of quantitatively and reproducibly evaluating photochromic colouration, photofading, and photo fatigue in scattering textile substrates, thereby bridging fundamental photokinetic with textile-specific optical complexity and applied durability assessment.

The thesis sets out and consistently achieves *four main objectives*: it develops a reproducible and quantitative methodology for measuring photochromic colouration, photofading, and photo fatigue in solid-state textile systems; establishes a unified kinetic framework for comparing different textile architectures such as surface-applied photochromic prints and bulk-dyed electrospun nonwovens; systematically investigates factors impacting photodegradation including *UV wavelength, irradiance, dose, dye concentration, textile architecture, temperature, oxidation, and measurement protocol*; and *proposes kinetic descriptors that remain meaningful*, scattering textile conditions. These objectives are not only well formulated but are also convincingly fulfilled. The thesis goes beyond empirical observation by developing conceptual and analytical tools that can be reused by the wider research community.

Chapter 2 is exceptionally comprehensive and critical, demonstrating the author's strong grasp of photochemistry, colour science, and textile physics. It cohesively integrates fundamental photochromic mechanisms (AB/ABC schemes), limitations of idealised 1st order kinetics in solids, textile-specific challenges such as diffuse reflectance, optical screening, and heterogeneous microenvironments, as well as previous attempts to characterise photochromic fatigue and durability. Notably, the review's major strength lies in its clear identification of methodological gaps especially the lack of harmonised kinetic descriptors and the over-interpretation of exponential models in heterogeneous solids with the author positioning his work as a response to these deficiencies and justifying the adoption of logistic models and dose-based fatigue descriptors, thereby providing a robust intellectual foundation for the thesis.

Chapter 3 clearly justified and meticulously controlled. The selection of a spiroxazine-based photochromic dye is apt, given its prevalence and known fatigue issues. Comparing screen-printed photochromic layers with mass-dyed electrospun nonwovens provides valuable insight into the influence of textile architecture and microenvironment. Employing poly(vinyl butyral) as the polymer matrix, along with an optional HALS stabiliser, is scientifically sound and consistent with prior research. Methodology strengthened by custom-built spectrophotometer including FOTOCHROM2 and FOTOCHROM3, which allow for precise regulation of UV wavelength (360 vs 380 nm respectively), irradiance, cycling protocols, and temperature. The use of diffuse reflectance converted to K/S values is justified by the inherently scattering nature of textiles. Overall, the experimental design exhibits excellent reproducibility, transparency, and metrological awareness.

This thesis makes a significant contribution through its measurement philosophy, treating K/S as an effective optical observable rather than a direct concentration, thus offering a scientifically responsible approach. Key strengths include the segmentation of photochromic cycles into exposure and decay phases, the use of log-time linearisation to distinguish colouration regimes, and the application of 4-parameter (4PL) and 5-parameter (5PL) logistic models for describing non-exponential thermal fading. Notably, photochromic prints display symmetric (4PL) decay, while nonwovens show asymmetric (5PL) decay, illustrating architecture-dependent kinetics. Overall, the kinetic descriptors developed are robust, transferable, and well suited for complex textile systems.

The thesis offers an insightful and balanced analysis of measurement challenges in photochromic textiles, highlighting key issues such as optical scattering and penetration depth, architecture-dependent irradiance distribution, protocol dependence (continuous versus interrupted cycling), non-exponential relaxation in heterogeneous environments, and the distinction between reversible photo-switching and irreversible photodegradation. Crucially, the author demonstrates that the measurement protocol itself significantly influences observed fatigue behaviour, with a critical evaluation of Modes A, B, and C providing valuable guidance for future standardisation.

The dissertation is underpinned by an excellent publication record, comprising six peer-reviewed journal articles published in respected journals including J. of Industrial Textiles, Fibres and Textiles, and Fibres & Textiles in Eastern Europe, a journal manuscript submitted to *RSC Advances*, as well as several international conference proceedings, including AUTEX; this scientific output clearly exceeds typical doctoral requirements and confirms the originality, impact, and independence of the work.

While the work is of high quality, a few points could be discussed constructively during the final defence:

1. Further clarification could be provided on the relative contributions of photooxidation, aggregation-induced quenching, and irreversible structural changes of the merocyanine form.
2. Although oxidation is addressed, the defence could briefly consider how controlled-atmosphere experiments (e.g., inert gas) might further isolate degradation pathways.
3. A short clarification on how changes in scattering architecture (e.g., fibre compaction or surface roughening) were distinguished from true chemical photodegradation would strengthen interpretation.
4. Discussion on how broadly the proposed kinetic framework can be extended to other photochromic dye families (e.g., naphthopyrans, spiropyrans…) would be welcome.

Overall, this dissertation represents a substantial and original scientific contribution to the field of photochromic textiles. It combines strong theoretical insight with careful experimental design and delivers practical, transferable tools for evaluating photochromic performance and durability. The thesis fully satisfies and, in many respects, exceeds the requirements for the award of the doctoral degree. The candidate demonstrates clear scientific independence, methodological innovation, and a strong publication record. The work is highly suitable for successful defence and merits commendation.

Therefore, I recommend the Ph.D. dissertation for the defence.

Reviewer

Aravin Prince Periyasamy., Ph.D.
Scientist, Biomass processing and products
VTT Technical Research Centre of Finland Ltd.
Tekniikantie 21, 02150, Otaniemi,
Espoo,
Finland

02.04.2026

Univerzita
Pardubice
Fakulta
chemicko-technologická

Dissertation Review

Title of the thesis: Factors Affecting the Measurements of Photochromic Materials

Author of the thesis: Utkarshsinh Bhupendrasinh Solanki, M. Eng.

At the outset, I must state that the submitted dissertation deals with a major problem in the field of so-called functional dyes, namely the photodegradation of photochromic dyes, which is currently still very rapid and thus prevents the large-scale use of these dyes in practice.

This submitted dissertation describes the photokinetics and photodegradation of textile photochromic systems prepared using a photochromic dye from the spiroxazine group.

Two production routes were studied: surface-applied photochromic prints prepared by screen printing; and mass-dyed photochromic nonwovens prepared by the electrospinning method with dye doping.

A spirooxazine–based photochromic dye was selected as the photoresponsive compound for both printed and electrospun systems. The dye (5–chloro–1,3,3–trimethylspiro[indoline–2,3'–[3H]naphtho[2,1b][1,4]oxazine]) was supplied not in the pure form, but in the form of powder in polymer matrix, where was also present the hindered amine (4–amino 2,2,6,6–tetramethylpiperidine) as the light stabilizer (HALS).

Two textile platforms were used to represent the principal architectural classes of photochromic textiles. For prints, a woven polyester/cotton blend (65:35) was selected as the substrate for the application. For electrospun nonwovens, a spun–bond nonwoven fabric served as a continuous collector and structural support during nanofibre deposition. Poly(vinyl butyral) served as the polymer matrix for electrospinning.

Subsequently, the author of this dissertation investigated the UV-controlled photokinetics and photodegradation of the prepared textile photochromic systems. Colorimetric characterization was performed using the FOTOCHROM3 (360 nm) and FOTOCHROM2 (380 nm) systems. Time profiles of spectral reflectance were recorded at the dominant absorption

wavelength of the colored state (570 nm) and converted into units of color intensity according to the Kubelka–Munk function (K/S), which allowed for quantitative comparison of complete photochromic cycles. A response-oriented, step-wise measurement methodology was developed to quantify photofading after reaching the photostability (photostationary) equilibrium state and to evaluate the influence of key photodegradation parameters, including dye concentration, preparation method, irradiation time and intensity, UV dose, number of irradiation cycles (photofatigue), environmental conditions, measurement scenario within the cycle, and spectral distribution of the excitation source power (360 nm vs 380 nm). The phases of photochromism (exposure, E) and thermal fading (decay/attenuation, D) were analyzed separately.

Right at the beginning of my review, I can state that the work is of high quality and beneficial, as it essentially connects several fields, namely textile engineering, photochemistry, dye chemistry, and computer techniques.

In terms of form, the work is well-written and with good graphics and contains all the chapters and essentials that a dissertation should have.

As for the content of the matter, I will have a few notes and comments here, which are not intended as reservations about the work, but so that my review contributes to the further development of this issue.

The photochromic dye used in this work "works according to the following scheme".

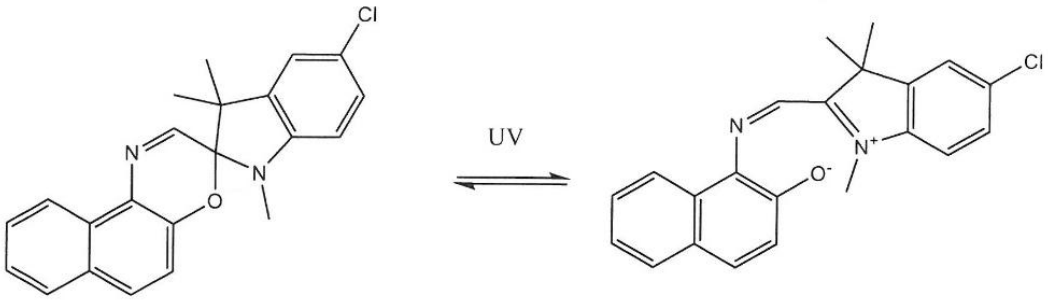

5-chloro-1,3,3-trimethylspiro[indoline-2,3'-naphtho[2,1-*b*][1,4]oxazine]
Chemical Formula: $C_{22}H_{19}ClN_2O$
Molecular Weight: 362,86

(*Z*)-1-(((5-chloro-1,3,3-trimethyl-3*H*-indol-1-ium-2-yl)methylene)amino)naphthalen-2-olate

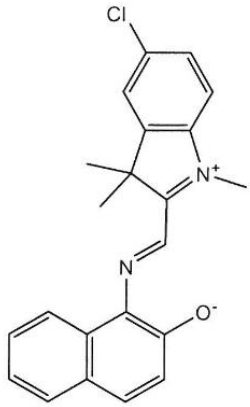

(*E*)-1-(((5-chloro-1,3,3-trimethyl-3*H*-indol-1-ium-2-yl)methylene)amino)naphthalen-2-olate
Chemical Formula: $C_{22}H_{19}ClN_2O$
Molecular Weight: 362,86

A colorless dye that absorbs UV radiation produces a merocyanine blue dye, which is in the form of a zwitterion, so that thermally (in the dark) it spontaneously returns to its original colourless form. An equilibrium is also established between the *Z* and *E* forms. The main problem with these dyes is that they easily form so-called triplets after absorbing radiation, which react with oxygen to form singlet oxygen, which not only oxidizes its surroundings, but this singlet oxygen also oxidizes the dye itself (attacks the -C=N- bond). Another fundamental problem is that the "open" blue form of the dye is the aforementioned zwitterion. This means that the reverse thermal reaction to the colourless closed form takes place only in "electrically neutral environments", hydrophobic materials (polymers). Manufacturers of photochromic dyes solve this problem by not selling pure dye, but powder, which is a hydrophobic polymer

coloured with a photochromic dye. And because hydrophobic polymers are subject to radical photooxidation under the influence of UV radiation, compounds called HALS (hindered amines light stabilizers) are added to these polymers, in this work:

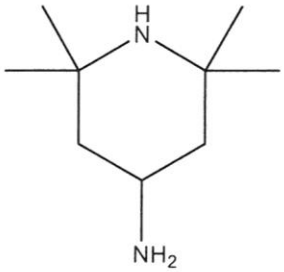

2,2,6,6-tetramethylpiperidin-4-amine

HALS work mainly through the so-called radical mechanism, they capture peroxy radicals (ROO•), capture alkyl radicals (R•), form nitroxyl radicals (R_2NO•) and thus interrupt autooxidation chains without consuming themselves. On the other hand, HALS react very little with singlet oxygen and are not primarily intended to react with singlet oxygen ($^1O_2$). This means that HALS do not prevent photooxidation of photochromic dye by singlet oxygen much. I mention this to make it clear how complex the problem is and how important it is to correctly set the technology for producing photochromic materials so that the stability of the system is as high as possible.

For the defence of the thesis, I have one recommendation that will contribute to a better presentation. Show the absorption (or transmission spectrum) of the starting material before irradiation, where the dye is in a closed form, and the spectrum of the material after irradiation, preferably how these spectra change over time during irradiation. And next to it, give the emission spectrum of the radiation source.

From these spectra it should then be clear that the system works in such a way that even open forms absorb radiation and the following diagram can be drawn, as presented by the author of the dissertation.

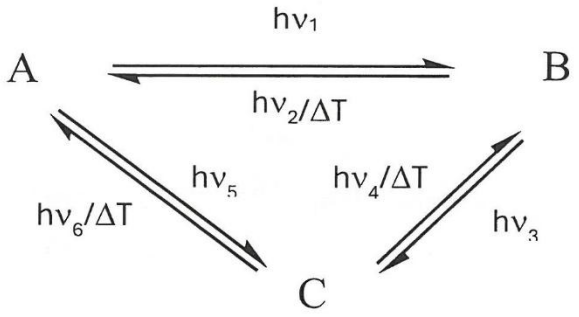

The initial closed form (A) is the most thermodynamically stable. When irradiated with UV light, the entire system starts to operate "cyclically", which explains the oscillations (Fig. 4.1.) in the curves of K/S dependence on the irradiation time log (t) (feedback mechanism).

The results of this work were published in 5 publications in impact journals and also presented at an international conference.

In conclusion, I am pleased to state that the student has demonstrated creative abilities in the given area of research and meets the requirements standard for dissertations in the field of Textile Engineering and I recommend the thesis for the defence and award of the Ph.D.

Pardubice on 22.3.2026

Prof. Ing. Radim Hrdina, CSc.
Institute of Organic Chemistry and Technology
Faculty of Chemical Technology
University of Pardubice